A thesis submitted to the University of Birmingham in partial fulfilment of the requirements for the degree of

MASTER OF RESEARCH

Neurotrauma and Neurodegeneration

School of Clinical and Experimental Medicine

&

School of Dentistry

University of Birmingham

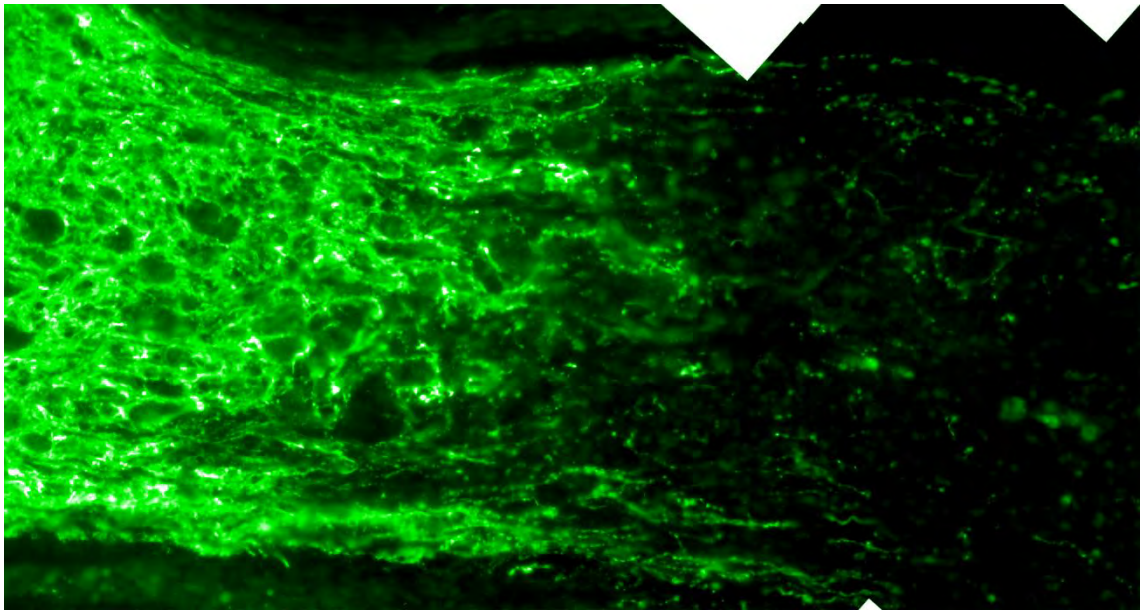

The pro-regenerative effects of dental pulp stem cells on the injured CNS

Ben Mead

Supervisors: Dr Wendy Leadbeater & Dr Ben Scheven

Acknowledgements

I would first like to thank my supervisors Dr Ben Scheven and Dr Wendy Leadbeater for their support and guidance throughout the whole project. I would also like to thank Prof Martin Berry for his help with the surgery, Maj Richard Blanch for his help with fundoscopy and Dr Jenna O'Neill for her help in the preparation and analysis of the optic nerves.

Finally, I would also like to thank the staff at the dental school and the Molecular Neuroscience Group at the medical school, for the friendly, welcoming atmosphere and providing help whenever needed.

Contents

List of figures

Abstract

Injury to the central nervous system (CNS) leaves patients with irreversible loss of critical functions such as vision and movement due to the limited regenerative capabilities of CNS axons. Stem cells offer two potential means of treating CNS injury, either differentiating into, and replacing lost neurons, or indirectly promoting the regeneration of endogenous injured neurons.

The aim of the present study was to determine the potential benefit dental pulp stem cells (DPSCs) could provide in CNS injury. Rat DPSCs were subjected to a three week differentiation medium to induce neuronal differentiation. DPSCs were also tested for their potential pro-regenerative capabilities in an *in vitro* (primary retinal ganglion cell (RGC) culture) and *in vivo* (optic nerve crush) CNS injury model.

DPSCs failed to differentiate into neurons following the three week inductive medium protocol. DPSCs, when cultured with primary RGCs, significantly increased the number of regenerating RGC neurites. When transplanted into the vitreous, DPSCs significantly increased both survival of RGCs and regeneration of RGC axons following optic nerve crush.

This study although unable to successfully differentiate rat DPSCs into neurons, reveals the potential of DPSCs as a candidate cellular therapy in treating CNS injury.

1 Introduction

1.1 CNS injury – the clinical problem

Injury to central nervous system (CNS) tissue is severely debilitating to the patient not only due to its critical role in sensory and motor function but also due to the post-mitotic state and regenerative capabilities of the tissue. The most common cause of CNS injury is through trauma with 130,000 people a year (reviewed in Thomas and Moon, 2011) suffering a spinal cord injury (SCI) and 80,000 a year (Ghajar, 2000) suffering traumatic brain injury which leads to severe, permanent neurological disability. Non-traumatic diseases can also affect the CNS such as glaucoma, a degenerative disease affecting the optic nerve which is the 2nd leading cause of blindness (Stone et al., 1997). Since the CNS is so functionally important, injury often leaves patients dependant on life-long care and unable to work or perform simple tasks and procedures. Thus, CNS injury can be seen as both debilitating to the patient and the economy and because of this, remains a huge research interest.

1.2 Regenerative capability of the CNS

Neurons, the cells residing in the nervous system which are responsible for the propagation of signals through the body, are post-mitotic. For this reason, neurons lost upon injury cannot be replaced. As well as the loss of irreplaceable neurons, CNS injuries also crush or sever axons (Figure 1), which in contrast to the peripheral nervous system (PNS), are incapable of regeneration. The lack of regenerative capacity of injured CNS axons can be attributed to both environmental changes associated with the injury response and intrinsic factors associated with CNS neurons.

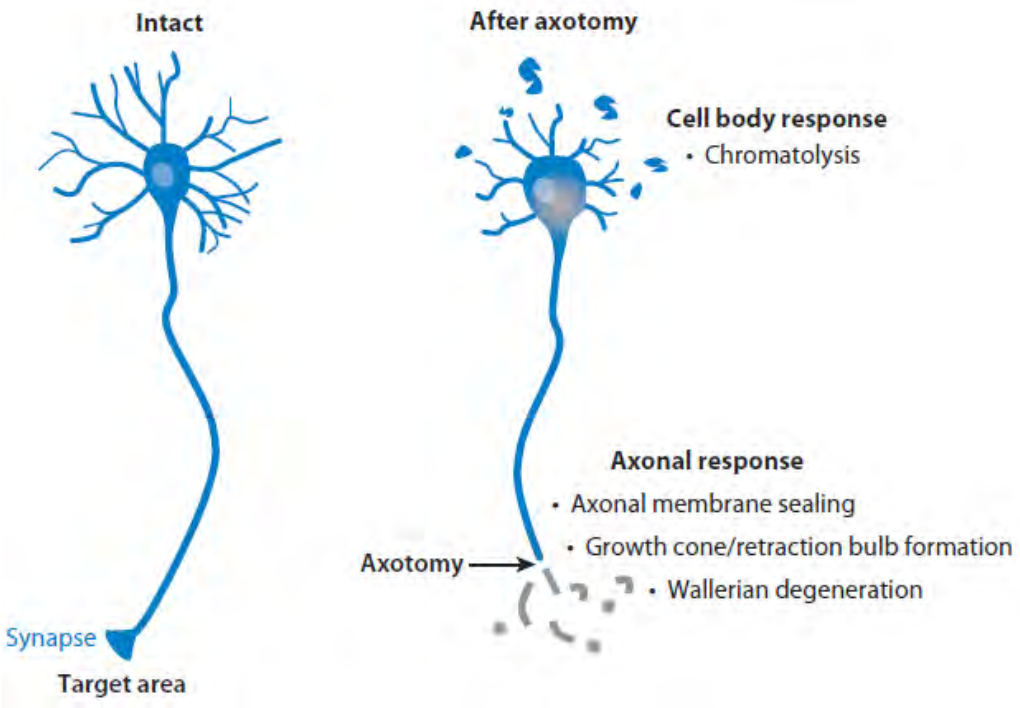

Figure 1: The neuronal response to axotomy is depicted. When the axon is severed, the distal segment begins degrading *via* a process known as wallerian degeneration; the remnants of this distal segment remain and stagnate in the environment. The proximal end reseals to prevent cytoplasm loss and in the case of the peripheral nervous system, which has a high regenerative potential, forms a growth cone. In the central nervous system however, proximal ends are only capable of limited abortive sprouting before the growth cone collapses. Cell bodies of the neurons also undergo chromatolysis, and without neurotrophic support and reconnection, die by apoptosis (Liu et al., 2011).

1.2.1 Regenerative capability of the CNS – extrinsic factors

The environmental importance was first revealed over 30 years ago by Richardson and Aguayo when they showed that an injured CNS axon could regenerate through a peripheral nerve implant (Richardson et al., 1980). This indicated for the first time that CNS axons are not incapable of regeneration and the non-permissive environment, the nerve which encapsulates the axons, is the limiting factor in their regenerative potential. This non-permissive environment has two important factors; a paucity of growth factors and an abundance of growth inhibitory molecules.

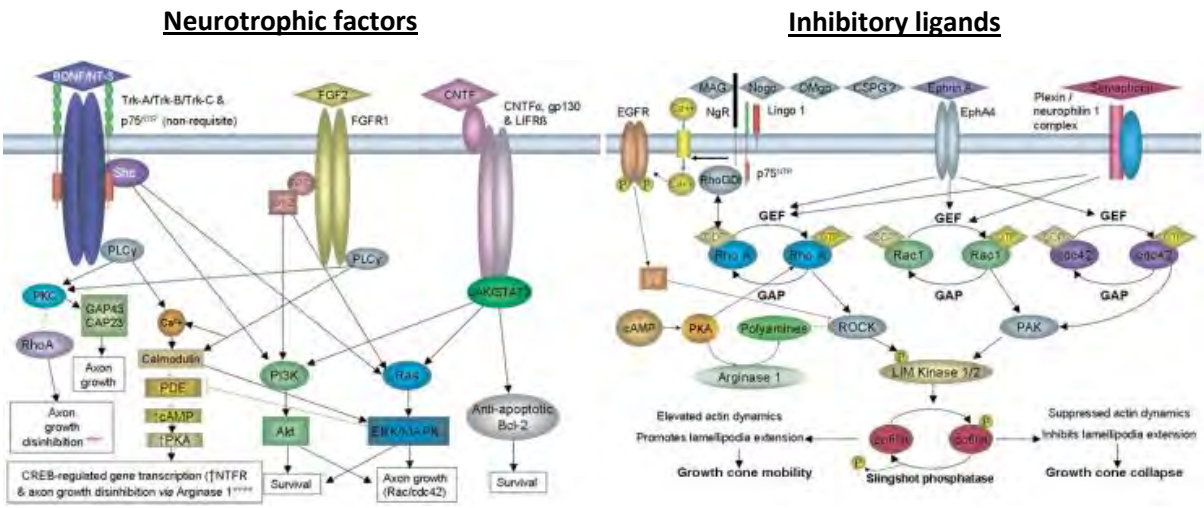

Figure 2: On the left, the typical signalling pathways that neurotrophic factors utilize to elicit their growth and survival promoting properties. On the right, growth inhibitory molecules signal through small GTPases to induce collapse of the growth cone and halt axon regeneration (Berry et al., 2008).

These growth factors, known as neurotrophic factors (NTFs) have a dual function; not only do they promote regeneration of axons but also act as potent survival factors for neurons (Figure 2). Neurotrophins, a type of NTF, consist of nerve growth factor (NGF), brain-derived growth factor (BDNF) and neurotrophic-3 (NT-3) which bind to the receptors tropomyosin receptor kinase-1, 2 and 3 (Trk) respectively (reviewed in Berry et al., 2008). They originate from the target organ, aiding in the generation of axons during development (Ernfors et al., 1994; Huang and Reichardt, 2001).

As well as a lack of growth factors, the presence of inhibitory ligands is also a considerable hurdle for axon regeneration (Figure 2). Schwab and Caroni showed in 1988 that CNS but not PNS myelin induced growth cone collapse of regenerating neurons *in vitro* and that antibodies raised against these proteins could prevent this (Caroni and Schwab, 1988; Schwab and Caroni, 1988). These proteins were later termed Nogo for their profound effect at inhibiting axon regeneration. Many other myelin-derived inhibitory ligands (MIL) have been revealed since and include myelin-associated glycoprotein (MAG) and oligodendrocyte-myelin glycoprotein (OMgp) (Benowitz and Yin, 2007); these can be found stagnating in the environment the distal axon occupied prior to injury (Figure 1). Myelin isn't the only source of inhibitory ligands however, these molecules, termed non-MIL, also play a significant part in preventing axon regeneration. The gliotic scar, which forms in the

injury site, is one source of these non-MIL which include ephrins, semaphorins (Berry et al., 2008), heparin-, dermatin-, keratin- and chondroitin sulphate proteoglycans (CSPGs) (Benowitz and Yin, 2007) which all inhibit axon regeneration.

1.2.2 Regenerative capability of the CNS – intrinsic factors

Although the extrinsic factors have received the widest attention, intrinsic factors are arguably of equal importance. The first intrinsic difference between neurons can be seen when comparing the neonatal spinal cord to the fully formed spinal cord. Injury to the spinal cord of a developing rat is met with robust and complete regeneration whereas after birth, post-injury regeneration fails (Liu et al., 2011). This is seen in other areas of the CNS, such as with the optic nerve with embryonic retinal ganglion cells (RGCs) extending axons at 10 times the speed of their mature counterparts. Thus, despite no drastic differences in the environment, intrinsic changes to neurons post-birth prevent regeneration following CNS injury.

One of the more well known intrinsic factors is growth associated protein-43 (GAP-43) which is expressed by neurons capable of robust regeneration and has been shown to have a causal role (Benowitz and Yin, 2007). RGCs when stimulated therapeutically to regenerate also show an almost ten times increase in GAP-43 expression (Benowitz and Yin, 2007), an association widely used when staining for regenerating axons. Another important intrinsic regulator of axon growth is the mammalian target of rapamycin (mTOR) pathway which is both down regulated following birth and further down regulated following axonal injury. Forced upregulation of this pathway by deletion of its negative regulator phosphatase and tensin homolog (PTEN) promotes robust axon regeneration (Park et al., 2008).

1.3 Stem cells as a potential treatment

As outlined above, CNS injury yields two avenues of potential treatment. The first is to promote endogenous repair mechanisms and limiting further cell death. This **indirect** approach owes its functional recovery to long distance axon regeneration, reconnecting the soma or cell body of the neuron to its original target. The second potential treatment can be seen as a more **direct** approach, replacing post-mitotic neurons lost during the injury. Stem cells, which can be extracted from an ever increasing list of sources (Figure 3), can be used in both of these approaches.

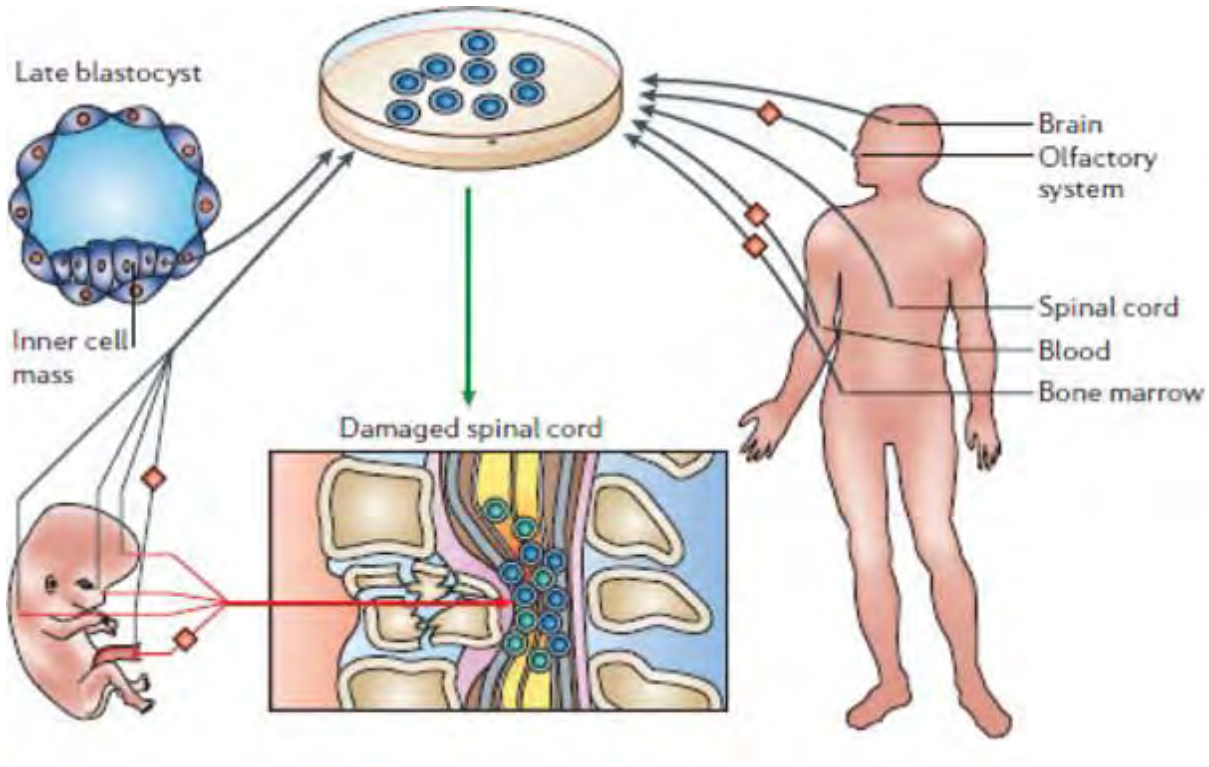

Figure 3: Potential sources of stem cells for transplanting into the injured spinal cord are shown. Stem cells can be isolated from a variety of different tissues and either transplanted directly into the lesion or differentiated in inductive medium prior to transplantation. Some sources such as olfactory system, blood, bone marrow and umbilical cord offer the potential for autologous transplantation (Thomas and Moon, 2011).

1.3.1 Stem cells as a potential treatment – direct support

The direct approach is what is most widely associated with stem cells in terms of treatment for CNS injury. Stem cells are unique in being the only source of primary neurons available for potential transplantation. Following transplantation, it is hoped that these neurons will form relays or "bridges" that injured axons undergoing endogenous local regeneration can branch onto, essentially,

reconnecting the circuit broken previously by the injury. Evidence for this occurring is strong; Bareyre et al showed in 2004 that in an untreated injury model of SCI, axons of the corticospinal tract (critical for movement) regenerated spontaneously formed new connections with undamaged propriospinal neurons (involved in sensing the surroundings) (Bareyre et al., 2004). These new connections acted as novel circuits, bridging around the lesion and contributing to functional improvement. This experiment shows the potential of both anatomical plasticity (sprouting of axons) and functional plasticity (upregulation or alteration of the function of neurons to improve function) with many studies reporting similar findings (Blesch and Tuszynski, 2009; Cafferty et al., 2008). This process occurring in humans is evident by the fact the 60-80% of individuals who have suffered a SCI regain some sensory or motor function, often over many years (Fouad et al., 2011).

(Moon and Bunge, 2005). Blocking inhibitory signals within the injured CNS environment also has been shown by countless experiments that alone, only promote minor axon regeneration (Benowitz and Yin, 2007). Perhaps the best axon regeneration seen to date is a combination of both extrinsic agents and forced intrinsic changes to the neurons (Kurimoto et al., 2010), exemplifying the need for a combinatorial therapy (multiple agents targeting different signalling pathways combined into one treatment).

Stem cells can act as local factories for a huge array of molecules which can alter the levels of both NTFS and MIL/non-MIL, producing a more permissive environment to axon regeneration. The advantage over conventional administration of axiogenic agents is that you get continuous production which has more of a chance of altering the environment then a single injection. Secondly, they can produce a wide array of different factors which is important in tackling the multifocal nature of the injury.

One study showed the potential of this by transplanting bone marrow-derived mesenchymal stem cells (MSCs) into a SCI site. They showed that although these MSCs didn't differentiate, they promote both axon regeneration and a reduction in lesion size (Gu et al., 2010). The authors attributed this to the fact that these MSCs expressed both BDNF and glial cell line-derived neurotrophic factor (GDNF).

1.4 Dental pulp stem cells

In 1999 it was shown by Harada *et al* that cells within the dental pulp are positive for BrdU, a marker of dividing cells (Harada et al., 1999). Dental pulp stem cells (DPSCs) were first isolated by Gronthos a year later in 2000 (Gronthos et al., 2000) using a plastic adherent assay and were shown to possess both self-renewal and multi-lineage differentiation capabilities, two defining features of stem cells. Three years later the same group published a paper reporting successful isolation of a stem cell population from human exfoliated deciduous teeth, referred to as SHED (Miura et al., 2003). These

cells had the same multi-lineage differentiation potential as DPSCs but proliferated faster suggesting they are similar to DPSCs but perhaps more immature.

DPSCs have been shown by multiple studies to express the mesenchymal marker STRO-1 (Gronthos et al., 2000) but not the hematopoietic marker CD45 (Miura et al., 2003; Sakai et al., 2012) and similar finding are seen in DPSCs from mice (Guimaraes et al., 2011). Other markers both SHED and DPSCs appear positive for include CD90, Nestin, GFAP and βIII-tubulin (Sakai et al., 2012). This however is controversial since the Gronthos group reports DPSCs are only positive for βIII-tubulin post-differentiation, not before (Arthur et al., 2008). Since many other markers appear to be differentially expressed depending on the lab doing the analysis, it can be considered that these cells have not be fully characterised as of yet.

1.5 The advantages of dental pulp stem cells

DPSCs have three advantages over other more widely researched stem cell sources. The first is that they are possibly more prone to forming neurons than other stem cells. This is because the majority of the tooth, including the dental pulp is derived from the neural crest (Chai et al., 2000) (Figure 6), the same neural crest (Figure 5) that forms neurons during development (Huang and Saint-Jeannet, 2004). Other stem cells on the other hand, do not form neurons, for example NSCs, which despite the name, rarely differentiate into neurons and instead form glial cells (Coutts and Keirstead, 2008).

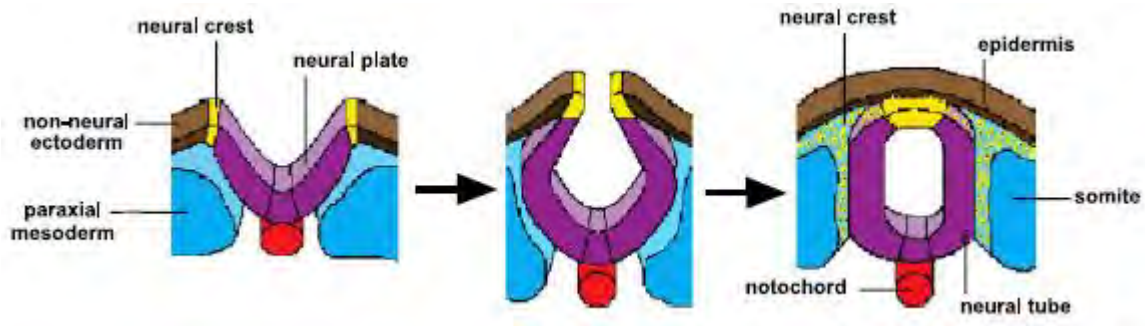

Figure 5: Neurulation is the folding of the neural plate to form the neural tube with the neural crest occupying the dorsal region of this tube. These neural crest cells migrate out to form other tissue such as peripheral neurons whereas the rest of the neural tube goes on to form the brain and spinal cord (Huang and Saint-Jeannet, 2004).

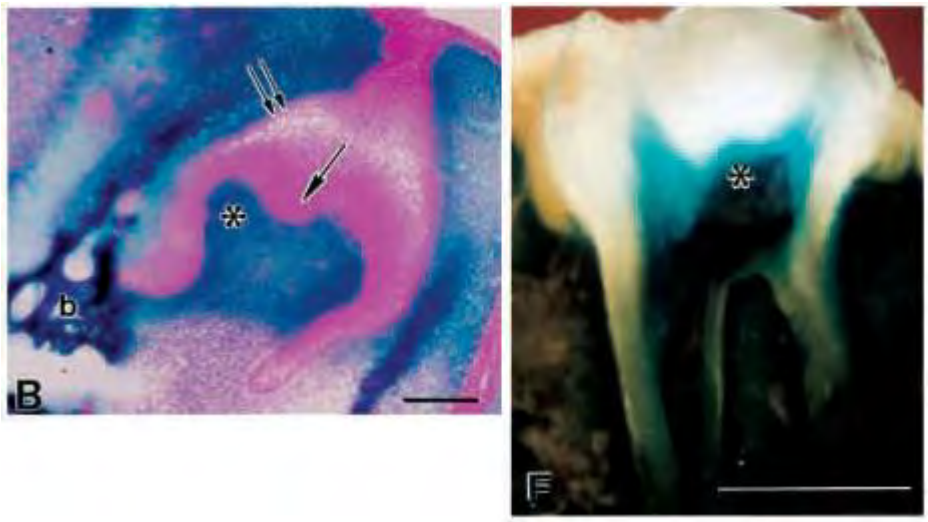

Figure 6: Transgenic mice expressing β-galactosidase in neural crest cells were used, allowing the fate of these cells to be mapped throughout development. On the left, a developing mouse tooth at embryonic day 15. The arrows, pointing to the inner and outer enamel epithelium, are comprised of β-gal negative cells, given by their pink appearance and thus, are not derived from cranial neural crest. The dental papilla (*) on the other hand is dark blue meaning β-gal positive and thus, derived from the neural crest. The dental papilla goes on to form both dentin and pulp in later stages of development. On the right, an adult mice tooth is shown, derived from the same transgenic mice. The pulp and dentin are both β-gal positive (*), thus being derived from neural crest. Scale bars for B and F represent 100µm and 500µm respectively (Chai et al., 2000).

The second advantage is that there are fewer ethical consideration than those which shroud other stem cells. Most notable is embryonic stem cells which, due to their blastocystic origin, can and is argued their use is ethically unjustified. This leads to a lack of support for this research and also a reduced number of patients willing to take any potential treatments discovered in the future .

Thirdly, they are more easily isolated than other stem cells such as MSCs from the bone marrow and NSCs from cadavers (Coutts and Keirstead, 2008). Since they are isolated from third molars or "wisdom teeth" (Arthur et al., 2008; Gronthos et al., 2000), widely considered vestigial organs, their extraction is no loss to the individual and can be expanded with ease or stored without detriment (Papaccio et al., 2006). This feature of DPSCs opens up the potential for autologous transplantation, removing the need for immunosuppressive therapy.

1.6 Model of CNS injury

To understand CNS injury, appropriate models are required, both *in vitro* and *in vivo*, which recapitulate the pathology that is seen in humans. Each model has its advantages and disadvantages

and varies from simple to complex. Most hypotheses driven research begins with the simple models and if promising, move forward to be put through more complex and rigorous injury models.

The most simple of these models is the *in vitro* RGC culture experiment (Logan et al., 2006). This experiment involves the extraction and culture of primary RGCs from an animal (usually a rat) and the quantification of both RGC survival and neurite growth under different treatment groups. Since the optic nerve which harbours the axons of the RGCs is severed in this model, it replicates the injury response seen after CNS injury.

Moving *in vivo*, the next simplest model is the optic nerve injury model. The optic nerve is a collection of CNS axons, all originating from the RGCs within the retina. For these reason it serves as an excellent model of CNS injury since all connections between RGCs and their targets can be severed at the lesion site and without disruption of the blood supply (Berry et al., 2008). Furthermore, a variety of experimental tools are available such as lens injury (to assess the effects of inflammation of axon regeneration) and fluorogold back labelling of RGCs (to accurately quantify cell death). Finally, because the cell bodies of the RGCs are directly adjacent to the vitreous, intravitreal injections are an easy and non-invasive way of delivering and assessing the efficacy of treatments to promote regeneration and RGC survival (Johnson et al., 2010; Logan et al., 2006).

The most complex of the *in vivo* models is the animal model of SCI. This model involves contusion or transection (complete or partial) of the spinal cord and can be localised to thoracic regions for disruption of hind limb function or the more severe cervical region for disruption of forelimb and respiration (Moon and Bunge, 2005).The advantages of this model is it more accurately replicates a SCI seen in humans. Unlike the optic nerve injury where RGCs are almost completely lost 3 weeks post lesion (Berry et al., 2008), neurons within the spinal cord remain relatively quiescent following injury, allowing investigators the ability to test the efficacy of drugs in the chronic phase rather than just in the acute phase (Moon and Bunge, 2005). Another advantage of this model is it allows locomotory function to be assessed using the gold standard BBB locomotor test (Basso et al., 1995).

This test has been shown to be reliable and accurate and allows comparisons with other treatments tested in other labs to compare efficacy. A drawback of this model is that because the spinal cord is a much more complex structure, “sparing” of axons can occur following injury giving the illusion of functional recovery following pro-regenerative treatment when infact, recovery is due to these spared axons. Another issue is that treatments may promote plasticity such as the sprouting of injured neurons onto other non-injured neurons or the potentiation of central pattern generators below the lesion site. These scenarios will lead to functional recovery and thus a higher BBB score without any long-distance axon regeneration taking place. A final disadvantage is the large reduction in animal well being and need for rigorous supervision and care.

1.7 Current research into DPSCs as a treatment for CNS injury – direct support

Human DPSCs have been shown by two groups to differentiate into neurons (Arthur et al., 2008; Kiraly et al., 2009). The first group, led by Stan Gronthos, used a three week inductive medium protocol to differentiate DPSCs into neurons which expressed neuronal markers, took on a neuronal morphology and expressed voltage-gated sodium channels (Arthur et al., 2008). The second paper published by Kiraly *et al* used a similar method to induce neuronal differentiation achieving similar results but these DPSC-derived neurons also expressed voltage-gated potassium channels (Kiraly et al., 2009). Currently only one study has taken this *in vivo* by transplanting DPSC-derived neurons into the cerebrospinal fluid (Kiraly et al., 2011). This study, published by the Kiraly group was a proof of principle rather than a measurement of efficacy and showed transplanted cells integrated into host brain and survived the duration of the study (four weeks). Interestingly, they also showed that transplanted cells preferentially integrated into injured regions of the cortex. Currently no protocol exists on the differentiation of rat DPSCs into neurons.

the injured spinal cord, preserving myelination. A similar study showed significant recovery of sensorimotor function following middle cerebral artery occlusion induced stroke when DPSCs were transplanted into the lesion site. The transplanted DPSCs differentiated into an astrocytes-like phenotype, rather than neurons, suggesting DPSCs contributed as a support cell *via* trophic factors (Leong et al., 2012).

1.9 Aims

The aim of this study is to explore the potential benefits of DPSCs in treating CNS injury, both directly and indirectly. To address the issue of a direct benefit, a protocol will be developed to reliably differentiate rat DPSCs into neurons based on information from the two papers that have reported this using human DPSCs (Arthur et al., 2008; Kiraly et al., 2009). Immunohistochemical and morphological differences will be used to assess DPSCs pre- and post-differentiation to determine if successful differentiation has occurred. Changes during successive passages will also be analysed.

To assess any potential indirect benefit, DPSCs will be co-cultured with RGCs and the pro-regenerative effects can be analysed *via* measurements of RGC neurite growth. If successful, DPSCs will be transplanted into the vitreous of a rat following optic nerve crush (ONC) with subsequent RGC survival and optic nerve regeneration measurements done to prove similar effects *in vivo*.

1.10 Hypothesis

Similar to human DPSCs, rat DPSCs can be successfully differentiated into neurons, providing the foundation for future *in vivo* work focused on transplanting DPSC-derived neurons into a SCI site.

Due to their production of NTFs and “blinding” of neurons to their disinhibitory environment, DPSCs will promote significant neurite outgrowth of RGCs *in vitro* and promote both regeneration of axons and survival of RGCs *in vivo* following ONC.

incisors. Incisors were transferred in α-MEM (Biosera, Ringmer, UK) supplemented with 1% penicillin/streptomycin (P/S) to the sterile conditions of a laminar flow hood. The posterior ends of the incisors were cracked open and then dental pulp removed. Dental pulp was sliced into pieces no bigger than $1mm^3$ using a scalpel blade and incubated in 4ml of 0.25% trypsin-EDTA for 30 minutes at 37°C. Trypsin was inactivated by adding an equal volume of α-MEM containing 1% P/S and 20% foetal bovine serum (FBS; Biosera). A single cell population was obtained by passing through a 70μm cell strainer (BD Biosciences, Oxford, UK). The cell suspension was centrifuged at 500 xg for 5 minutes. Pellets were resuspended in 1ml of α-MEM containing 1% P/S and 20% FBS and seeded onto a T25 flask (Corning, Amsterdam, NL) at a total volume of 5ml. Medium was changed every 3 days and cells were passaged when 70% confluent and cultured at 37°C, 5% CO_2.

2.3.2 Fibroblast cell culture

Mouse fibroblast 3T3 cells were provided frozen in liquid nitrogen at passage 22 by Gay Smith. Cells were defrosted on a 40°C hot plate for 2 minutes before being seeded on a T75 flask (Corning) in α-MEM containing 1% P/S and 10% FBS. Medium was changed every 3 days and cells were passaged when 90% confluent.

2.3.3 Retinal ganglion cell/dental pulp stem cell co-culture

Cell culture 8-well chamber slides (BD Biosciences) were prepared by incubating for 90 minutes with poly-D-lysine (100μg/ml) and then 30 minutes with laminin (20μg/ml). Cell suspensions of either DPSCs (at passage 2) or fibroblasts, both obtained *via* the protocol above were pelleted, resuspended and plated in each well at a seeding density of 20,000cells/well and incubated for 24 hours at 37°C in 300μl of supplemented neurobasal-A (24.2ml neurobasal-A (Life Technologies, Gibco, UK) supplemented with 500μl of B27 supplement (Life Technologies, Invitrogen, UK), 62.5μl of L-glutamine (200mM; Invitrogen) and 125μl of gentamycin (Invitrogen)).

The following day eyes were obtained from male Sprague-Dawley rats weighing 250g (Charles River) and the retinae dissected out. Retinae were minced in 1.25mls of papain (Worthington Biochem, NJ, USA) containing 62.5µl of DNase I (Worthington Biochem) and incubated for 90 minutes at 37°C. Following this incubation the tissue suspension was centrifuged at 300 xg for 5 minutes and the pellet was resuspended in a solution containing 1.35ml of EBSS (Worthington Biochem), 150µl of reconstituted albumin ovomucoid inhibitor (Worthington Biochem) and 75µl of DNase I. This cell suspension was then added on the top of 2.5ml of albumin ovomucoid inhibitor to form a discontinuous density gradient and this was centrifuged at 70 xg for 6 minutes. The resulting pellet was resuspended in 1ml of supplemented neurobasal-A and seeded on top of the DPSCs/fibroblasts at a seeding density of 125,000. CNTF (200ng/ml) or the Trk receptor inhibitor K252a (50nM) was used in some cultures to assess the importance of NTFs in the co-culture. The co-culture was incubated for 4 days at 37°C before staining *via* immunocytochemistry.

2.3.4 Neuronal differentiation of DPSCs

Differentiation of DPSCs towards a neuronal lineage was done based on the method given in the 2008 paper by Arthur *et al* (Arthur et al., 2008). Cell culture 8-well chamber slides were prepared by incubating for 90 minutes with poly-L-ornithine (10µg/ml) and then 30 minutes with laminin (20µg/ml). DPSCs at passage 2 were seeded into the chamber wells at a density of 5000, 10000 and 20000 and allowed to expand in α-MEM containing 1% P/S and 10% FBS for 3 days. After 3 days DPSCs were cultured in supplemented neurobasal-A containing 20ng/ml EGF (Peprotech EC, London, UK) and 40ng/ml bFGF (Peprotech) for 1 week. After 1 week the medium was changed to DMEM:F12 containing 1X insulin-transferrin-sodium selenite solution (ITSS; Roche, Burgess Hill, UK), 40ng/ml bFGF and 1% P/S. For the 3rd week DPSCs were cultured in DMEM:F12 containing 1X ITSS, 40ng/ml bFGF, 1µm retinoic acid, 0.5mM dcAMP and 1% P/S. Controls were DPSCs left in α-MEM containing 1% P/S and 10% FBS for 3 weeks.

2.4 *In vivo* experiments

All surgical procedures were carried out under Home Office guidelines in accordance with animal act 1986 (UK) and after local ethical approval (BERSC). Prof Martin Berry performed the ONC and cell injections whereas Rhodamine-B-isothiocyanate (RITC) injections and perfusions were performed by myself. Anaesthesia was provided by either myself or Lisa Hill. Animals were kept in a well-controlled environment (21°, 55% humidity) in a building adjacent to the laboratory. Animals were given food/water *ad libitum* and kept under a 12 hour light and dark cycle while under constant supervision from well trained staff. Four female Sprague Dawley rats weighing 200-250g (Charles River) were used for this experiment, treatment groups given in Figure 9. For anaesthetic induction 5% Isoflurane/1.5L per minute O_2 was used with Isoflurane being lowered to 3.5% prior to surgery. The pedal reflex was used to assess animal sedation prior to surgery.

Beginning 3 days prior to the surgery and maintained for the duration of the study, cyclosporin A was used as an immunosuppressant to prevent rejection of transplanted cells. Administration was *via* the drinking water at a final concentration of 100µg/ml. This was under the assumption that the rats will drink 20mls a day and thus provide them with the effective amount of 10mg/kg/day. Fluid intake was monitored throughout the study to confirm this assumption.

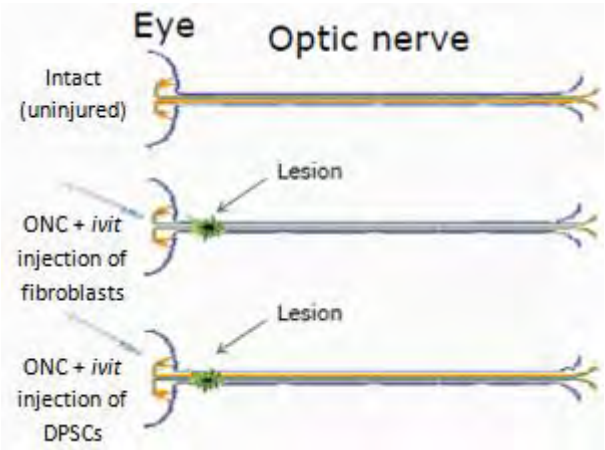

Figure 9: The three treatment groups are shown on the left with each group consisting of an n of 4. Data derived from intact eyes, analysed in exactly the same way, was readily available. The middle treatment group consisted of an optic nerve crush (ONC) and intravitreal (*ivit*) injection of 400,000 fibroblasts, both on day 0. The bottom treatment group consisted of an ONC and an *ivit* injection of 400,000 dental pulp stem cells (DPSCs), both on day 0. Animals were sacrificed on day 21.

2.4.1 Intravitreal injections

Following anaesthesia, animals had analgesia administered subcutaneously (buprenorphine 0.1ml/mg) before their heads were shaved and secured in a head-holding frame. Isoflurane administration was maintained at 3.5% throughout the surgery. The head was rotated 45° so the eye to be injected is in the superior position. Using angled, non-toothed forceps in the left (non-dominant) hand the eye was gently exhumed from the socket up to the point where the circumference of the limbus can be seen. A sterile cotton bud was used to apply pressure to the corner of the eye to aid in exhuming it from the socket. Forceps were tightened briefly to keep the eye rigid while minimising the time spent with a compromised blood supply. A glass micropipette produced from glass capillary rods (Harvard apparatus, Edenbridge, Kent, UK) using a Flaming-Brown micropipette puller (Sutter instruments, California, USA) was preloaded with 400,000 cells suspended in 10µl of phosphate-buffered saline (PBS), either fibroblasts or DPSCs, to be injected into the left and right eye respectively. Injections were done at the angle shown in Figure 10 and to relieve ocular pressure, the eye was injected with a needle tip at a point 180° from the original injection site.

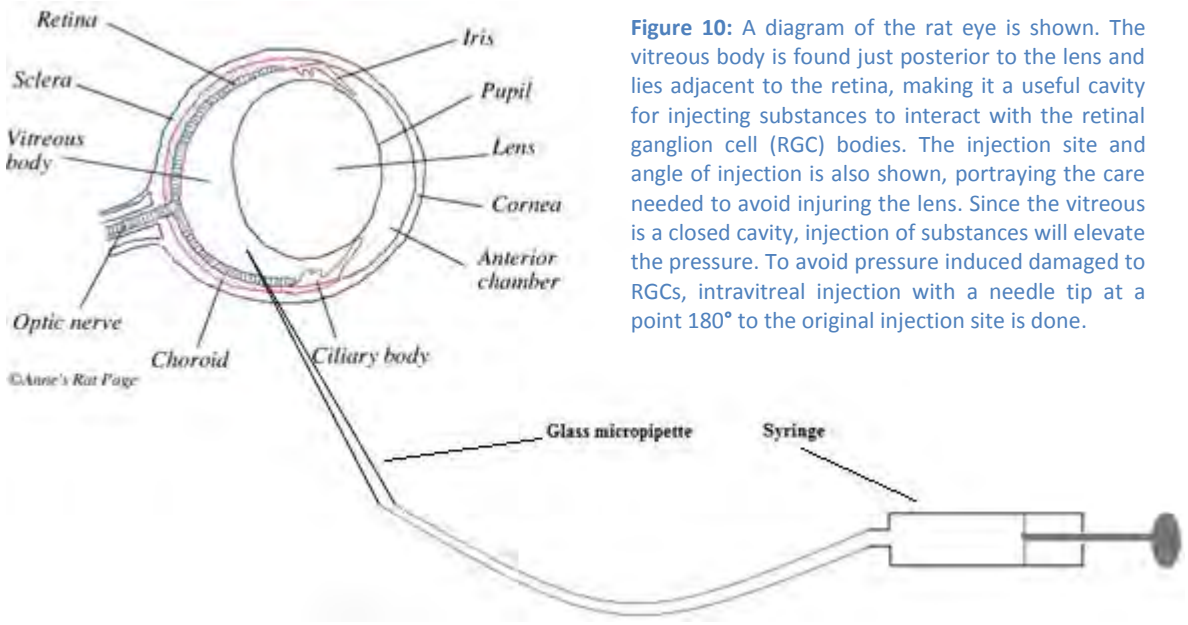

Figure 10: A diagram of the rat eye is shown. The vitreous body is found just posterior to the lens and lies adjacent to the retina, making it a useful cavity for injecting substances to interact with the retinal ganglion cell (RGC) bodies. The injection site and angle of injection is also shown, portraying the care needed to avoid injuring the lens. Since the vitreous is a closed cavity, injection of substances will elevate the pressure. To avoid pressure induced damaged to RGCs, intravitreal injection with a needle tip at a point 180° to the original injection site is done.

2.4.2 Optic nerve crush

ONC was performed concurrently with intravitreal injections with maintained anaesthesia as above. Using blunted scissors and toothed forceps a midline incision was made along the scalp. Using fine forceps the skin was retracted, and loose connective tissue was separated until the temporal and supraorbital ridge were visible. Using the top blade of fine scissors the temporalis muscle was cut with a vertical incision. The temporal ridge was cut along in a caudally fashion whilst avoiding the ophthalmic vein. After identification of the neurovascular bundle, both ends were clamped and cut. The harderian gland was separated from its capsule and to prevent it from moving back a sterile tissue strip was placed in the way. The retractor bulbi muscle was removed and a 2nd sterile tissue was placed on the opposite side of the first to isolate and visualise the optic nerve. The dural sheath that surrounds the optic nerve was removed and the nerve itself, crushed using forceps at the point 2mm from the optic nerve head. Following surgery, animals were sutured and placed in a heated recovery cage. Ten days into the study, animals were examined using fundoscopy with the help of Maj Richard Blanch.

2.5 Tissue preparation

At the end of the study animals were sacrificed by rising concentrations of CO_2 and immediately after, fixed by intracardiac perfusion with 4% paraformaldehyde (PFA; TAAB, Reading, UK) in PBS with concurrent clamping of the descending aorta to limit perfusion to the head region.

2.5.1 Dissection

Eyes were dissected out by cutting around the orbit, separating the eye from the oblique/rectus muscles and finally, the optic nerve at the posterior side of the eye. To dissect out the optic nerve, skin from the head was peeled anteriorly to reveal the skull and subsequently, bone clippers were

2.5.4 Immunohistochemistry

Sections were allowed to equilibrate to room temperature before being hydrated in PBS for 2 X 5 minutes. After washes, tissue was permeabilized in 0.1% triton x-100 in PBS for 20 minutes at room temperature. Tissue was washed for 2 X 5 minutes in PBS and isolated with a hydrophobic PAP pen (Immedge pen; Vector Laboratories, Peterborough, UK). The tissue was blocked (75µl; 0.5% bovine serum albumin (g/ml), 0.3% Tween-20, 15% normal goat serum (Vector Laboratories) in PBS) in a humidified chamber for 30 minutes at room temperature. After the 30 minutes block, tissue was incubated with primary antibody diluted in antibody diluting buffer (ADB; 0.5% bovine serum albumin, 0.3% Tween-20 in PBS) overnight at 4°C. The following day slides were left to equilibrate with room temperature for 20 minutes before being washed in 3 X 5 minutes of PBS. Tissue sections were then incubated with secondary antibody diluted in ADB for 1 hour in a hydrated incubation chamber at room temperature. After the 1 hour, slides were washed in 3 X 5 minutes of PBS, mounted in vectorshield mounting medium containing DAPI (Vector Laboratories) and stored at 4°C prior to microscopic analysis.

2.5.5 Immunocytochemistry

Cells were fixed in 4% PFA in PBS for 10 minutes and then washed in 3 X 10 minutes of PBS at room temperature. Cells were next blocked in blocking solution for 20 minutes at room temperature followed by incubating with primary antibody diluted in ADB for 1 hour at room temperature. After the 1 hour, cells were washed in 3 X 10 minutes of PBS and incubated with the secondary antibody diluted in ADB for 1 hour at room temperature. The cells were then washed in 3 X 10 minutes of PBS and mounted in vectorshield mounting medium containing DAPI and stored at 4°C.

2.6 Analysis

2.6.1 Microscopy

Analysis of the immunohistochemically and immunocytochemically stained sections was done using Zeiss Axioplan-2 fluorescent microscope (Carl Zeiss Ltd, Hertfordshire, UK). For immunocytochemistry, RGC counts were done in real-time on the microscope incorporating the entire slide. Neurite growth measurements were done by taking images at 20X magnification using Axiocam HRc camera and Axiovision software (Carl Zeiss Ltd). Each chamber well was separated into 9 equal regions and an image of each region was taken, focussing on the largest neurite growth of each region. Images were then converted to Tiff format ready for analysis. *In* vitro RGC neurite length was measured using Image Pro Analyzer 6.2 (Media Cybernetics inc, Bethesda, MD, USA). Data quantification was done blind with the treatment groups unbeknownst to the experimenter at the time of quantification.

For immunohistochemistry, RGC counts were done on 20µm thick sections of the retina. Four sections per animal were used and 4 animals per treatment group. Sections were chosen in the same plane by ensuring the optic nerve was visible and counts were done in a 250µm region, either side of the optic nerve. Counts from intact eyes, quantified using the same method, were already available from a previous study. For *in vivo* quantification of axon regeneration, 20X magnification images were taken along the optic nerve and a composite image was created using Photoshop CS3 (Adobe Systems inc, San Jose, CA, USA). Using these images, RGC axon regeneration was quantified by counting the number of GAP-43 positive axons extending across a line set at 100µm, 200µm, 400µm, 800µm and 1200µm from the crush site (identified by laminin^{+} staining). By using the thickness of the nerve at each measurement point, the number of axons/mm width was derived. This value was then used to derive $\sum ad$ (the total number of axons extending distance d in an optic nerve with

radius *r*) *via* the formula below (where *t* is the section thickness (0.015mm)). This was done for 3 animals for each treatment, 2 sections per animal.

$$\sum ad = \pi r^2 \times \frac{\text{average number of axons/mm width}}{t}$$

2.6.2 Statistics

Kolmogorov-Smirnov test was used to ensure all data was normally distributed prior to parametric testing. After verifying suitability of parametric testing, paired and independent T tests were used to test for statistical significance in cases with 2 treatment groups. Where multiple treatment groups were present, a one-way analysis of variance (ANOVA) with a Tukey post-hoc test was used. Levene's test was used for assessing whether equal variance could be assumed and hence, the correct P value chosen. Significant difference was taken at P values of less than 0.05.

3 Results

3.1 Overview

DPSCs are positive for glial fibriliary acidic protein (GFAP), nerve growth factor receptor (NGFR-P75) and nestin. Following the three week differentiation protocol, DPSCs lost their nestin expression and ubiquitously, although very weakly, up-regulated βIII-tubulin expression.

When co-cultured with RGCs, DPSCs promote significant neurite outgrowth compared to fibroblasts which acted as controls. Blocking of the NTF receptor using K252a completely reversed this DPSC-induced growth potentiation. When transplanted into the vitreous, DPSCs promoted a significant increase in RGC survival and RGC axon regeneration following ONC.

3.2 DPSCs have the potential to provide direct support during CNS injury

The immunocytochemical staining profiles of DPSCs at passage 0, 2 and 4 are given in figure 11. DPSCs are positive for GFAP and negative for βIII-tubulin with the exception of a very small amount of cells which showed weak positivity for βIII-tubulin (Panel A). These βIII-tubulin positive cells were lost rapidly after subsequent passages (Panel D and G). DPSCs are weakly positive for NGFR-P75 and negative for myelin basic protein (MBP) and this observation was unaffected by passage number. Finally, subpopulations of DPSCs are positive for nestin which became more apparent with increasing passage number (Panel I).

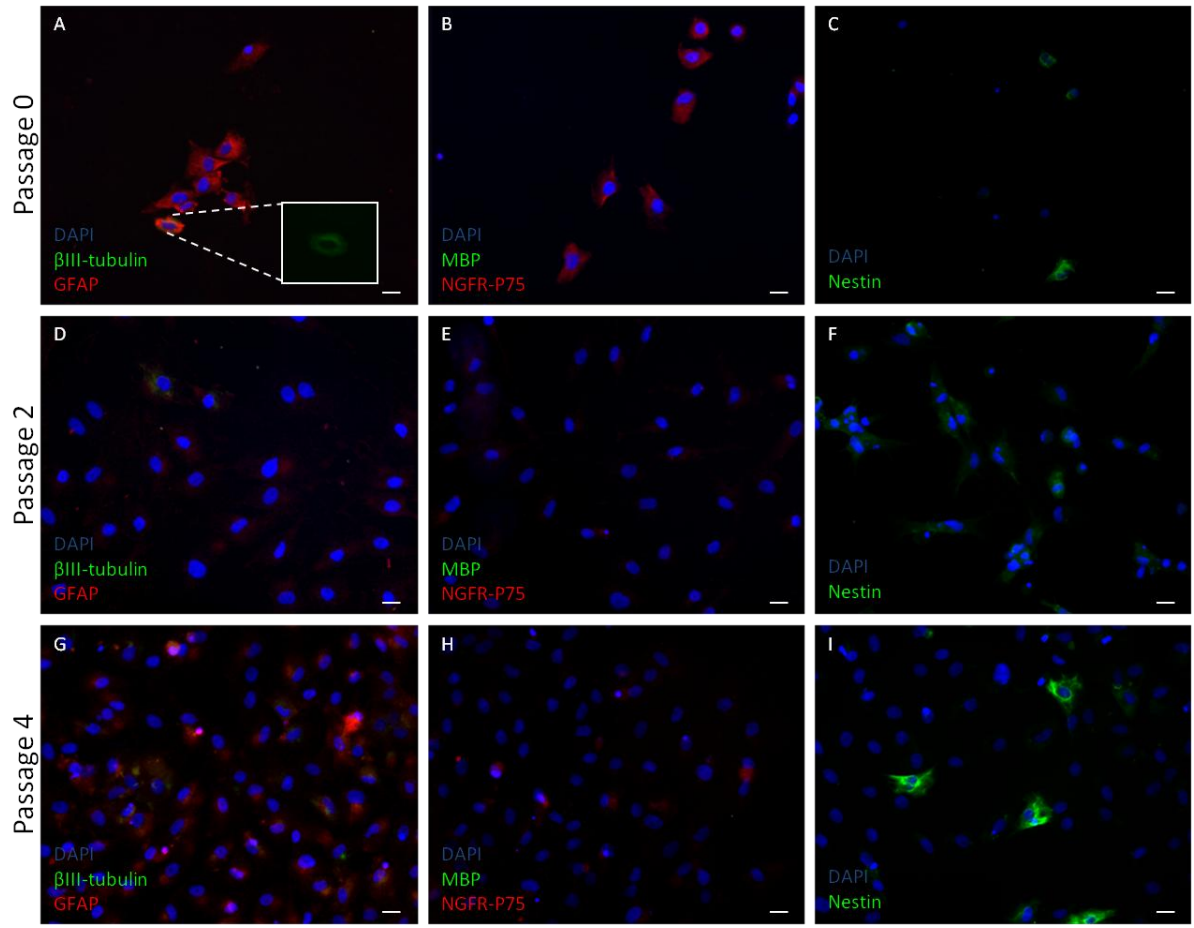

Figure 11: Immunocytochemically stained cultures of dental pulp stem cells (DPSCs) at passage 0 (A-C), passage 2 (D-F) and passage 4 (G-I). All images are representative of the entire culture. DPSCs were stained for βIII-tubulin and glial fibriliary acidic protein (GFAP; A, D and G), myelin basic protein (MBP) and nerve growth factor receptor (NGFR-P75; B, E and H), and nestin (C, F and I). In all cases, DAPI was used as a counter stain. The insert in panel A shows a βIII-tubulin positive cell (GFAP staining removed). Scale bars represent 50µm.

Following differentiation (Figure 12), DPSCs maintained their strong GFAP expression (panel A). Expression βIII-tubulin could be seen in the majority of cells (Panel B) however intensity was very weak compared to mature neurons (Figure 13, Panel E). DPSCs remained positive for NGFR-P75 expression and negative for MBP expression (Panel C). Nestin expression was absent following differentiation (Panel D). The control experiment for the differentiation is given in figure 11 (Panel G, H and I). These DPSCs, at passage 4, spent three weeks in regular growth medium as opposed to three weeks in differentiation medium.

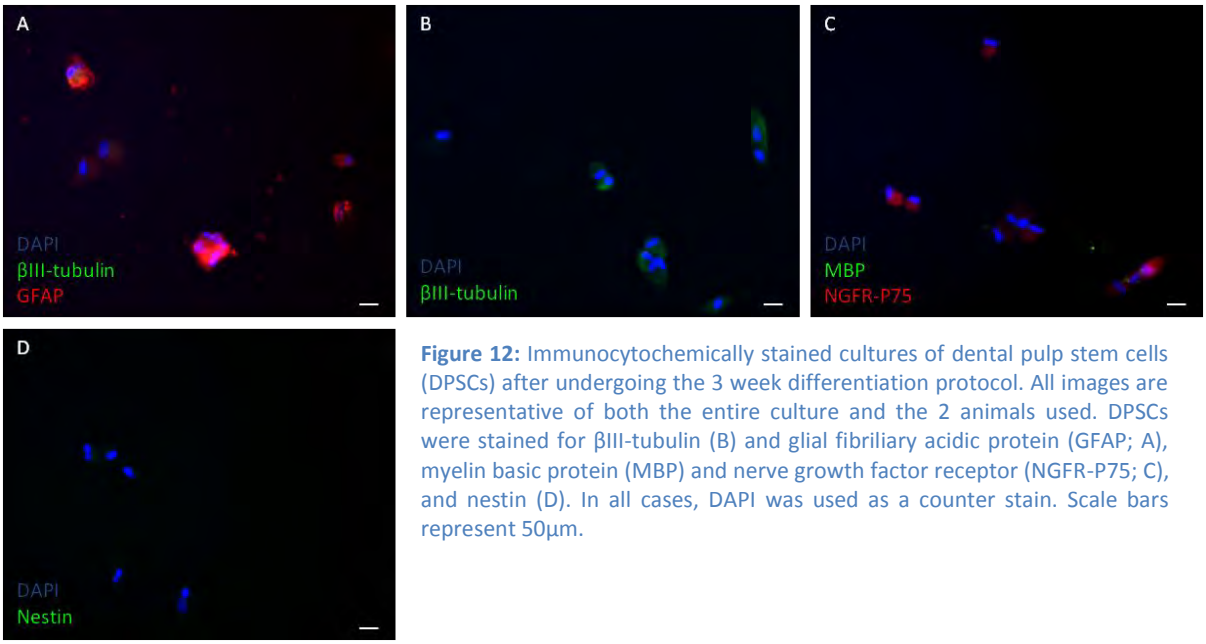

Figure 12: Immunocytochemically stained cultures of dental pulp stem cells (DPSCs) after undergoing the 3 week differentiation protocol. All images are representative of both the entire culture and the 2 animals used. DPSCs were stained for βIII-tubulin (B) and glial fibriliary acidic protein (GFAP; A), myelin basic protein (MBP) and nerve growth factor receptor (NGFR-P75; C), and nestin (D). In all cases, DAPI was used as a counter stain. Scale bars represent 50µm.

Figure 13 contains various staining controls. Panel A, B and C are fibroblasts stained with the antibodies used in this study and act as a negative control by showing the absence of staining. Panel D is another negative control whereby the primary antibodies are omitted, the lack of staining ensures the secondary antibodies have no direct specificity for the cells. Finally panels E-H act as positive controls, using retinal cultures which contain a collection of both neuronal and glial cells that are positive for the antibodies used.

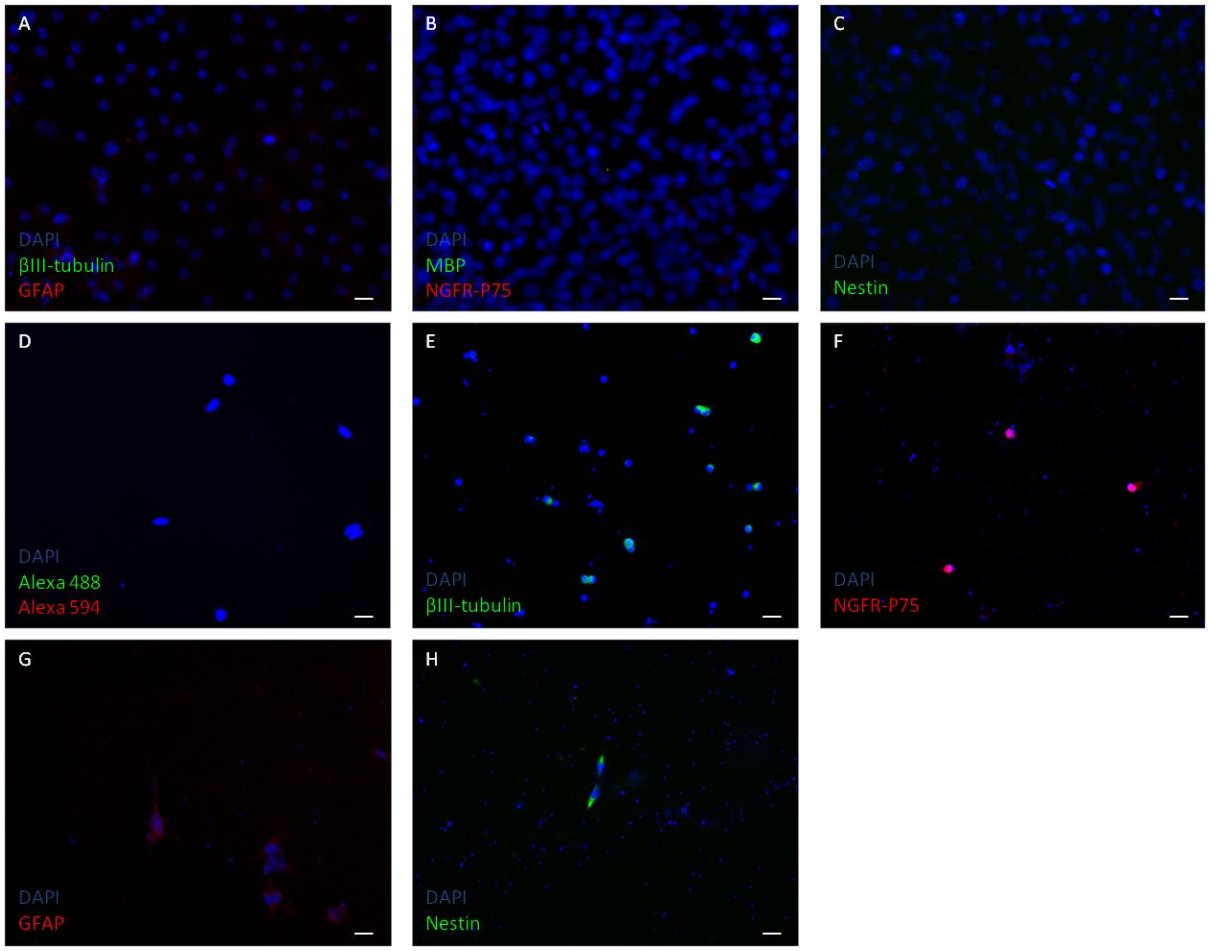

Figure 13: Immunocytochemically stained cultures of fibroblasts (A-C) dental pulp stem cells (DPSCs; D) or retinal ganglion cells (RGCs; E-H). All images are representative of the entire culture. Fibroblasts acted as negative controls and were stained for βIII-tubulin and glial fibriliary acidic protein (GFAP; A), myelin basic protein (MBP) and nerve growth factor receptor (NGFR-P75; B) and nestin (C). As a further negative control, DPSCs were stained with both primary antibodies omitted (D). Retinal cultures were used as primary controls for βIII-tubulin (E), NGFR-P75 (F), GFAP (G), and nestin (H). In all cases, DAPI was used as a counter stain. Scale bars represent 50µm.

3.3 DPSCs can provide indirect support during CNS injury

DPSCs, when co-cultured with RGCs promoted a significant increase in the percentage of RGCs regenerating neurites (49.9%) compared to either RGCs alone (21.6%) or RGCs cultured with fibroblasts (24.8%; Figure 15A). The addition of CNTF to the co-culture of DPSCs and RGCs did not significantly increase the percentage of regenerating neurites (51.9%) compared to the co-culture of only DPSCs and RGCs (49.9%). A similar trend could be seen when analysing the length of neurites instead of number, although no significance was reached (Figure 15B).

K252a, a blocker of the NTF receptors Trk-1, 2 and 3, significantly decreased both the percentage (11.3%) and length (16µm) of regenerating neurites seen when added to the DPSC/RGC co-culture

(Figure 15) compared to co-culture of DPSCs and RGCs alone (49.9% and 118.9µm respectively). Although cultures of RGCs alone or with fibroblasts showed some decrease in their number/length of regenerating neurites following the addition of K252a, this was not significant. Representative images of cultures from the different treatment groups that were used in the quantification are shown in figure 14.

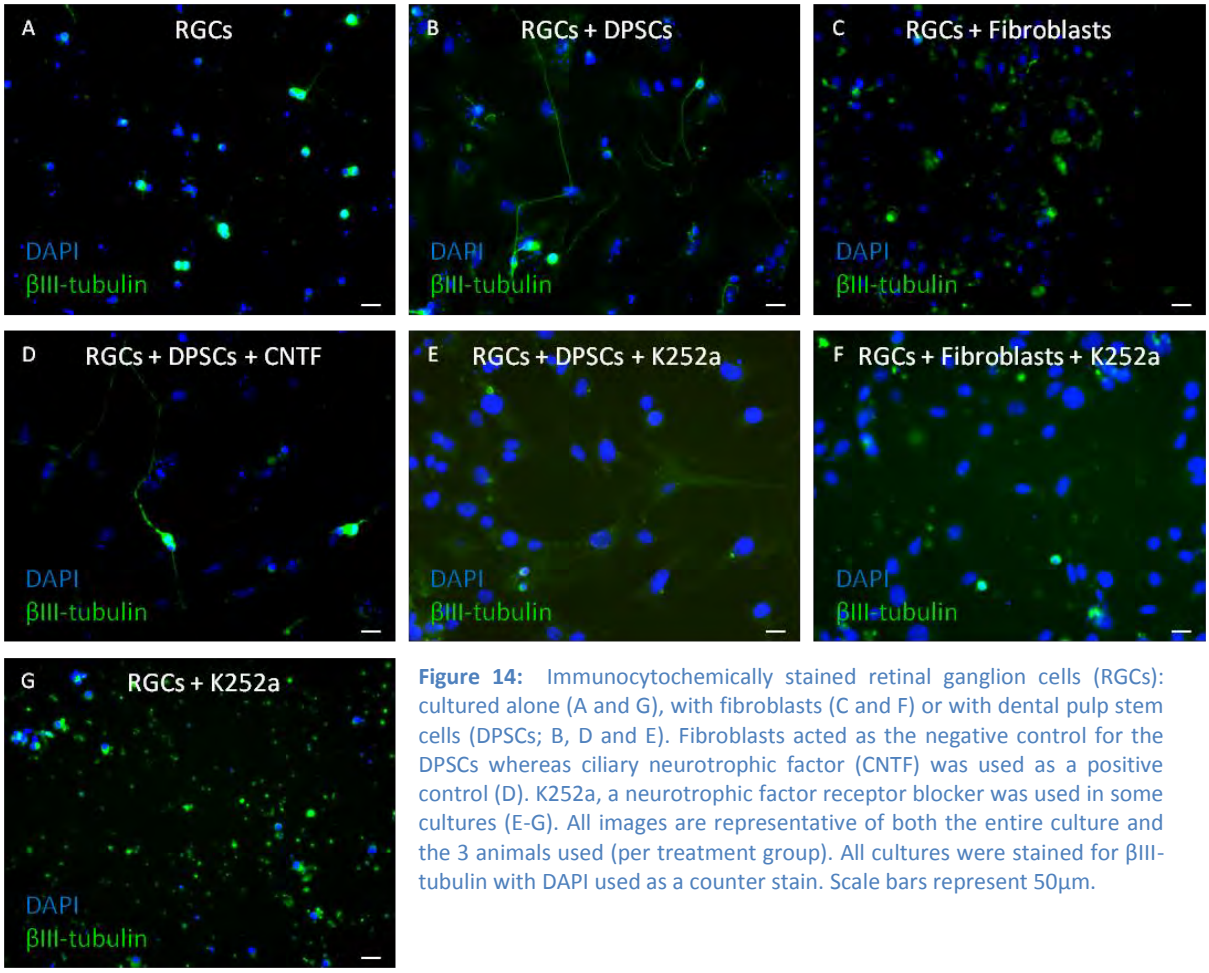

Figure 14: Immunocytochemically stained retinal ganglion cells (RGCs): cultured alone (A and G), with fibroblasts (C and F) or with dental pulp stem cells (DPSCs; B, D and E). Fibroblasts acted as the negative control for the DPSCs whereas ciliary neurotrophic factor (CNTF) was used as a positive control (D). K252a, a neurotrophic factor receptor blocker was used in some cultures (E-G). All images are representative of both the entire culture and the 3 animals used (per treatment group). All cultures were stained for βIII-tubulin with DAPI used as a counter stain. Scale bars represent 50µm.

DPSCs isolated from male rats, when injected into the vitreous of female rats, survived for the duration of the study (21 days). Transplanted cells were detected *in vivo* through the use of an antibody to the Y chromosome (Figure 16, Panel D and E). DPSC transplantation promoted a significant increase in the survival of RGCs (39.9 RGCs per mm of retina) following ONC compared to fibroblast treated (26.0 RGCs per mm of retina), as shown in the graph of figure 16. Both treatment groups however still suffered significant RGC death compared to uninjured eyes (87.7 RGCs per mm

of retina). Example images from each treatment group are given in panel A and B with the negative control in panel C.

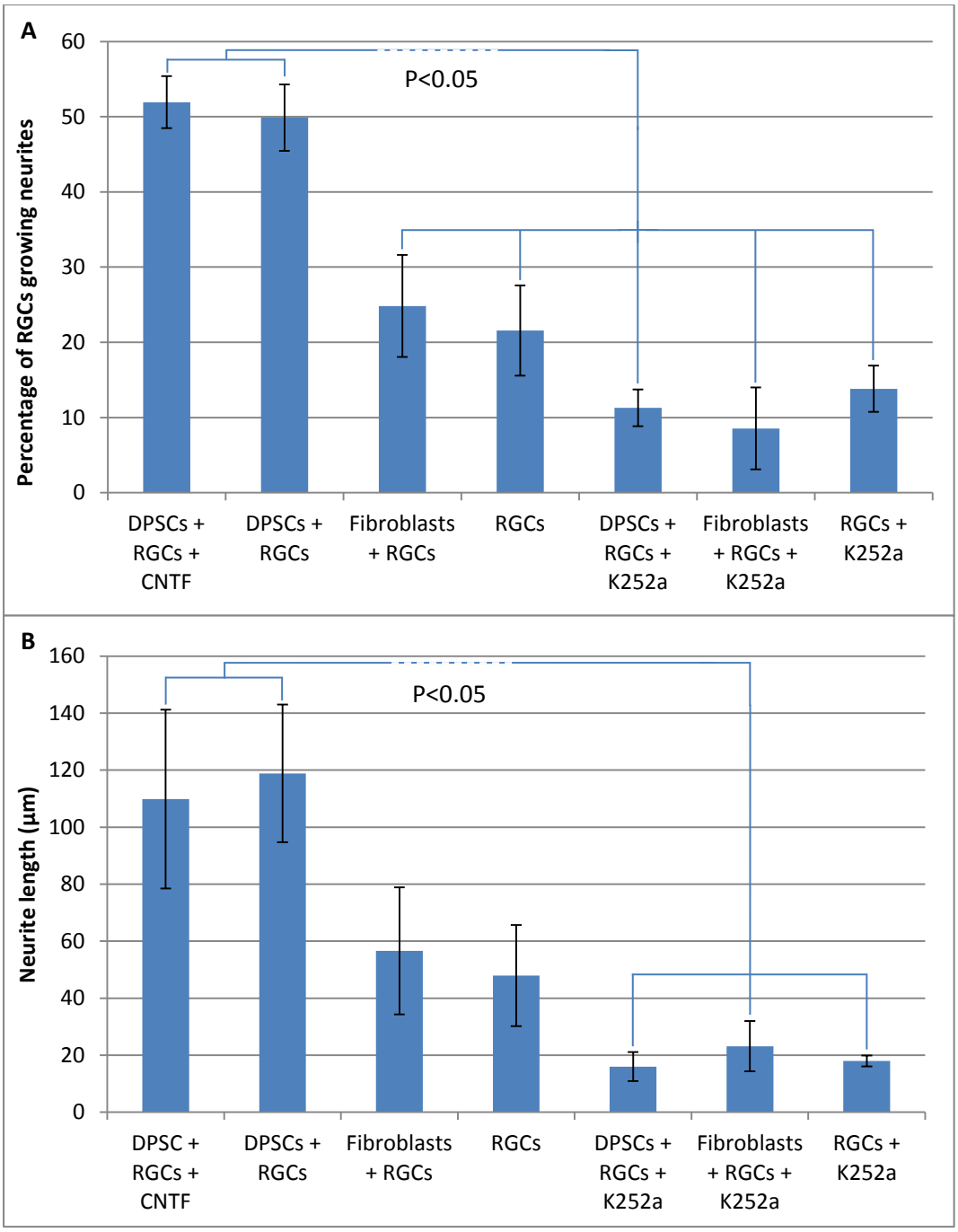

Figure 15: Graph A shows what percentage of the total numbers of retinal ganglion cells (RGCs) in each culture condition were growing neurites. Graph B shows, of these growing neurites, the average length of the longest. This average length was taken by dividing each chamber well into nine and measuring the nine longest neurites, one per division. All treatment groups used three animals. Error bars represent one standard error mean. Blue lines represent significant difference at P<0.05. Abbreviations: DPSCs, dental pulp stem cells; RGCs, retinal ganglion cells; CNTF, ciliary neurotrophic factor.

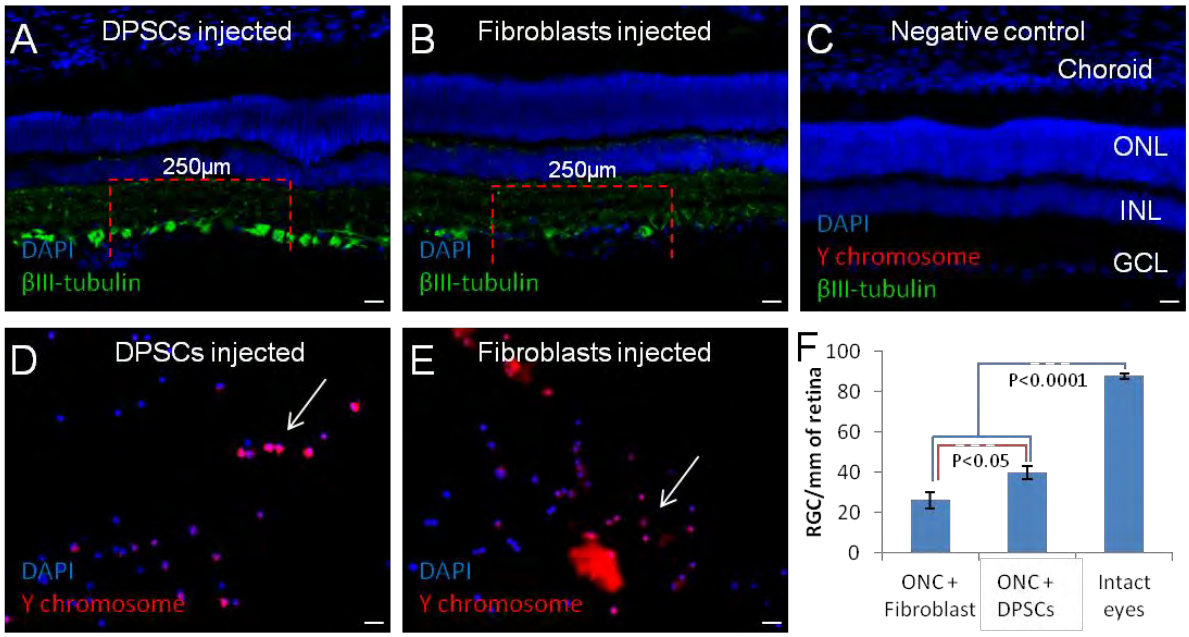

Figure 16: Immunohistochemically stained 20µm thick sections of retina are given above (A-E). Injected cells were detected using an antibody to the Y chromosome. Dental pulp stem cells (DPSCs; D) and fibroblasts (E) could be detected within the vitreous in the experimental and control eyes, respectively (white arrows). To quantify retinal ganglion cell (RGC) survival, cells positive for both DAPI and βIII tubulin were counted in a 250µm region of the RGC layer of the retina (A and B). A negative control were the primary antibody was omitted is included (C) with the choroid, outer nuclear layer (ONL), inner nuclear layer (INL) and ganglion cell layer (GCL) labelled. All images are representative of both the 4 sections per animal used, and the 4 animals per treatment group. In all sections, DAPI was used as a counter stain. Scale bars represent 50µm. The histogram (F) shows the number of RGCs in the retina of animals following optic nerve crush (ONC) and cell transplantation. RGC counts for intact eyes are also given however data is from a separate, earlier study. Error bars represent one standard error mean. Red lines represent significant difference at P<0.05 whereas blue represents significant difference at P<0.0001.

Regenerating RGC axons, identified in optic nerve sections by GAP-43 staining, extended across the lesion site in DPSC transplanted animals (Figure 17). Animals that received DPSCs had more axons positive for GAP-43 at regions both proximal (Figure 17, A and B) and distal (Figure 17, C and D) to the crush site. Quantification of the number of GAP-43 positive axons at various distances from the crush site is given in Figure 18. At all measured distances from the crush site, animals who received DPSCs showed a significantly higher number of regenerating axons.

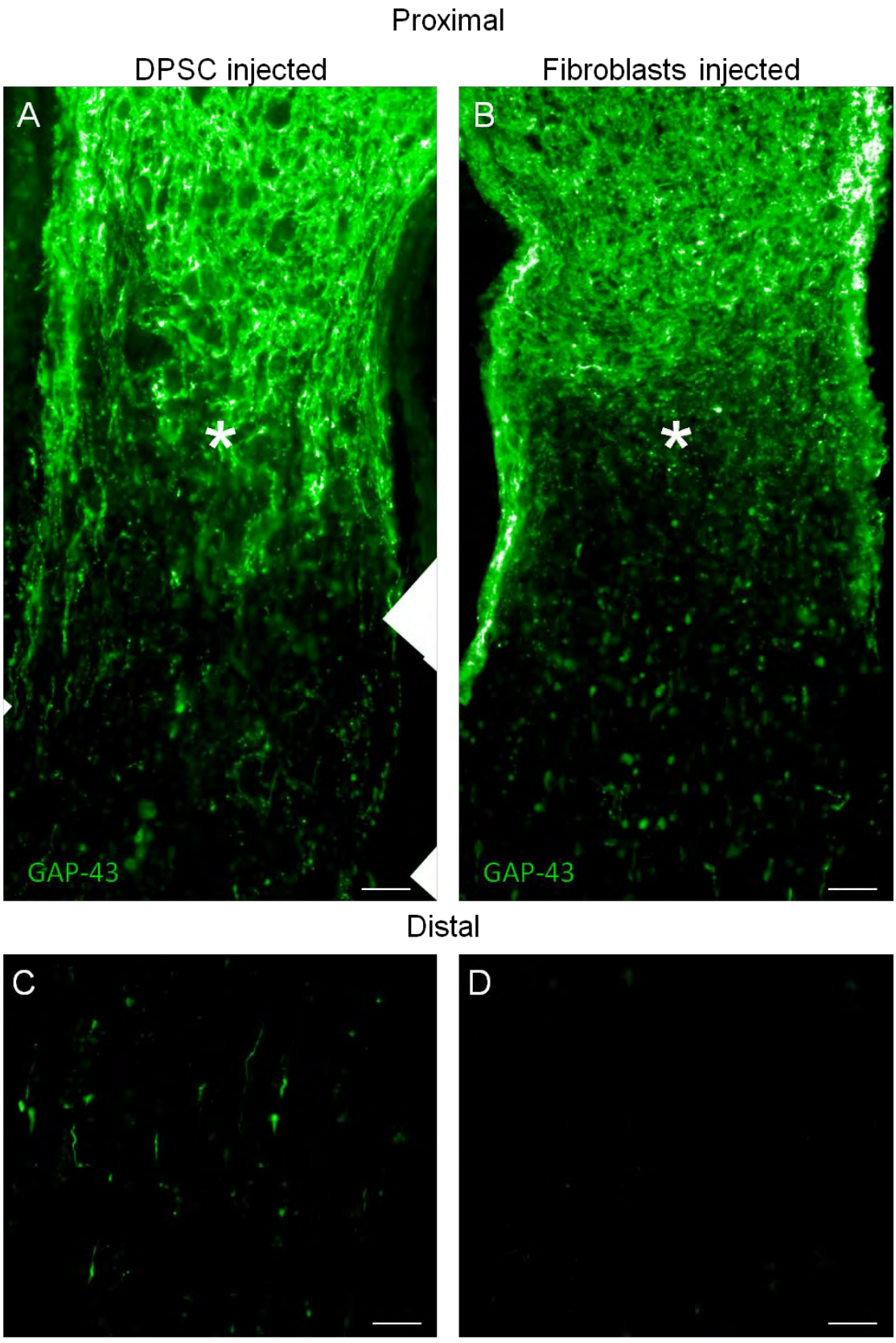

Figure 17: Immunohistochemically stained sections of optic nerve, 21 days after optic nerve crush. Treatment consisted of intra-vitreal transplantation of either dental pulp stem cells (DPSCs; A and C) or fibroblasts (B and D). Sections were stained for GAP-43. Images display both the crush site (A and B; crush site signified by a *) and 2mm distal to the crush site (C and D). All images are representative of the 3 animals used (per treatment group), 2 sections per animal. All images are composites of 4-8 images. Scale bars represent 100µm.

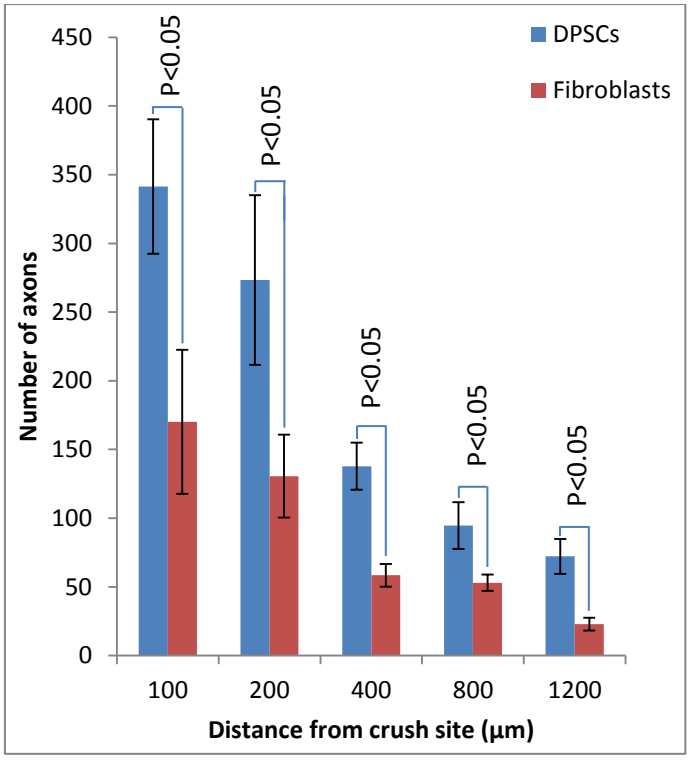

Figure 18: The number of regenerating axons in the optic nerve, identified through positive staining for GAP-43, is given at various distances from the crush site. Blue bars signify animals that received dental pulp stem cells (DPSCs) whereas red bars signify animals that received fibroblasts. Error bars represent one standard error mean. Blue lines represent significant difference at P<0.05.

4 Discussion

4.1 Overview

DPSCs failed to differentiate into neurons following administration of an inductive medium. DPSCs significantly increased the neurite outgrowth of primary RGCs in an *in vitro* co-culture assay. When transplanted into the vitreous of rats following an ONC, DPSCs promoted significant increase in both RGC survival and axon regeneration.

4.2 Differentiation of dental pulp stem cells into neurons

Differentiation of DPSCs into neurons was determined by detecting changes in protein expression *via* immunohistochemistry. To detect changes, it was thus first important to characterise the DPSCs in their undifferentiated form. Three separate points were chosen (passage 0, 2 and 4) since it is well known that MSCs undergo changes following subsequent passages (Nombela-Arrieta et al., 2011) and has even been reported that DPSCs take on a more restricted differentiation potential following repeated passages (Yu et al., 2010).

Since DPSCs have not been fully characterized, conflicting data exists on what proteins these cells are positive for. Some studies show DPSCs are strongly positive for βIII-tubulin and nestin both before and after differentiation (Sakai et al., 2012). The Gronthos group on the other hand found DPSCs to be largely negative for βIII tubulin, only increasing following differentiation (Arthur et al., 2008). The current study appears to agree with this notion; however, we observed a select population of DPSCs positive for nestin whereas the Gronthos group found all DPSCs isolated were positive for nestin. Since the isolation procedure was largely the same this could be due to a difference in species, since rat was used in this study whereas they used human.

Overall, it is unwise to say differentiation has occurred due to small changes in protein expression, especially considering the scientific community are conflicted on what proteins DPSCs express in

even their undifferentiated state. We could speculate that the loss of nestin expression is indicative of neuronal differentiation however considering survival of cells was poor in the differentiation medium, it may equally be selective death of nestin positive cells following administration of the inductive medium. Finally, no neurite expression was seen in these cells which are a key morphological characteristic of neurons, providing further evidence that neuronal differentiation did not occur in this study.

4.2.1 Future work

It is imperative to determine that any supposed DPSC-derived neurons are functional i.e. can fire an action potential. This, tested *via* patch clamp, has been done in a couple of studies (Arthur et al., 2008; Kiraly et al., 2009) and would need to be done as future work in this study for adequate proof of neuronal differentiation by determining the presence of functional voltage gated channels. Only when this is proven can it be taken *in vivo*, transplanting DPSC-derived neurons into a SCI animal model and measuring functional recovery through the BBB locomotory test (Basso et al., 1995), as has been done with MSC-derived neurons (Cho et al., 2009).

It is arguable that the above is getting ahead of a more important matter which is the characterisation of DPSCs. When some studies show DPSCs are positive for βIII-tubulin (Sakai et al., 2012) and other use βIII-tubulin expression as proof of differentiation (Arthur et al., 2008), it becomes apparent that full characterisation of these cells, taking into account different isolation methods and different species, is imperative. Only when you know what you are starting with can the differentiation potential of these cells begin to be mapped.

4.3 The supportive role DPSCs can provide following CNS injury

As mentioned previously, a study published early this year showed the positive effect stem cells isolated from the teeth can have on CNS injury (Sakai et al., 2012). The improvement in locomotory function following cell transplantation into a SCI occurred in the absence of neuronal differentiation. Various observations such as remyelination and improved axon regeneration were given in the study. The present study used RGCs as a model of CNS injury, both *in vitro* and *in vivo*, which as discussed earlier, is an effective method of quantifying regeneration.

When co-cultured with DPSCs, RGCs elicited a significant increase in neurite expression. This significance was seen in the number of RGCs expressing neurites, but not in the length of neurites. Despite the lack of significance in the latter measuring technique, a similar trend was seen to that in the former measuring technique. It is likely that the lack of significance is due to the greatly reduced sample size used when measuring neurite length, as opposed to counting all RGCs that are growing neurites.

This regenerative response was attenuated in the presence of K252a, a blocker of the NTF receptors. This is in agreement with recent evidence that shows DPSCs expressing a wide array of different NTFs (Sakai et al., 2012). Since the augmented regeneration was absent when K252a was added, the experiment strongly suggests that DPSCs promoted regeneration of RGC neurites through their secretion of these NTFs. Since the addition of CNTF provided no extra benefit, it is likely that RGCs had already reached a point of saturation in terms of NTFs *via* the DPSCs, meaning that the limiting factor in regeneration is through other pro-regenerative mechanisms.

NTFs possess another important characteristic which is the pro-survival effect on neurons. Axotomy removes a neurons supply of NTFs and thus the neurons subsequently dies. Quantification of RGC survival was not done in the co-culture assay due to the variability in RGCs that would seed down around the DPSCs. Variation in DPSC survival, division rate, size and seeding density meant the area

of the laminin coated chamber free for RGCs to grow on was varied between experiments. Thus, although quantifying regeneration was possible by calculating as a percentage of total RGCs, total RGC counts was an unreliable measure of cell survival, likely more reliant on the above factors.

Although RGC survival was not quantified *in vitro*, it was done *in vivo*. Following ONC, RGCs begin dying after five days and around 80-90% are dead following three weeks (Berry et al., 2008), thus making this a suitable model to assess survival. Our method for quantifying survival relied on counting RGCs (βIII-tubulin positive cells in the RGC layer) in a select region however slight variations in sectioning and embedding technique and a small sample (in relation to the whole retina) mean the method is inferior the gold standard fluorogold technique (Berry et al., 2008).

RGC survival was quantified and found to be significantly higher than control eyes that received fibroblasts instead of DPSC transplantations. This is in agreement with the study that transplanted DPSCs into the SCI of rat and showed reduced numbers of cells undergoing apoptosis (Sakai et al., 2012). Two other studies have shown significant RGC survival follow intravitreal cell transplantation. The first using mesenchymal stem cells in an animal model of glaucoma (Johnson et al., 2010), and the second using fibroblasts genetically modified to express NTFs in an ONC animal model (Logan et al., 2006). Both studies showed significant survival and both attributed this effect to the release of NTFs by the transplanted cells. There was however, still substantial RGC death (over 50%) which is seen in many studies at these timeframes, even those using caspase inhibitors (Ahmed et al., 2011). This aspect of the study would benefit from two improvements, dedicating animals purely for RGC survival analysis (i.e. using fluorogold) and secondly, quantifying RGC death at an earlier time point as well as three weeks. Another minor criticism is that the RGC count data from intact eyes was from an earlier study using male rats whereas the present *in vivo* study used female rats. With no reported difference in RGC numbers between male and female rats however, we did not consider it ethically justified to repeat that portion of the experiment.

Due to the promising neurite outgrowth results from the *in vitro* co-culture, it was hypothesised that a similar response would be seen *in vivo* with the ONC model. As expected, when transplanted into the vitreous, DPSCs promoted a significant increase in regenerating axons at all distances measured. GAP-43 was used to identify regenerating axons which is currently the gold standard for quantifying axon regeneration (Berry et al., 2008). The regeneration seen mimics other studies using intravitreal cell transplantation to promote axon regeneration (Logan et al., 2006). As well as more pronounced regeneration at the proximal stump, the distal region also showed significantly more GAP-43 positive axons, an important observation considering full long distance axon regeneration is required to restore function. It is these long distance regenerating axons that likely contributed to the restoration of function seen in the study transplanting DPSCs into a SCI (Sakai et al., 2012).

Despite regeneration occurring, the distance and quantity of regenerating axons is not as significant as some recent papers that use combinatorial strategies (Kurimoto et al., 2010). Due to this it is likely that DPSCs are promoting regeneration through the NTFs they release but by no other means and thus not in a combinatorial fashion. A future experiment would be to block the NTF receptors *in vivo* following DPSC transplantation, much like what was done for the *in vitro* experiment and determine if this is the only means by which they promote regeneration. Another possible way regeneration occurred is through triggering an inflammatory response since inflammation is a well known strong potentiator of axon regeneration (Benowitz and Yin, 2007). This however is unlikely since animals were on immunosuppressants and control animals that received fibroblast transplantations would also be expected to have an inflammatory response if this was the case. Another interesting experiment is to compare DPSC with other tooth-derived stem cells such as SHEDs. A future consideration is whether fibroblasts are a suitable control for the DPSCs or whether freeze-thawed DPSCs would be better. The primary issue with comparing DPSCs to control dead DPSCs is you are comparing dividing cells to non-dividing cells. It is thus desirable to use both fibroblasts and dead DPSCs as two separate controls. Rat fibroblasts rather than mouse fibroblasts should also be used in future experiments.

Despite their apparent monotherapeutic mode of action however, DPSCs represent a continuous, maintained source of NTFs, evident by the fact they are still present within the eye 21 days post-transplantation. A future analysis would be to determine survival rate of DPSCs following transplantation which may reveal if a second "booster" injection is required at some desired time point in the study. One future experiment would be to combine DPSC transplantation with another long term therapy, but intrinsic rather than extrinsic, such as genetic deletion of *pten* to determine any synergistic effects. A second future experiment would be to see if transplantation of DPSCs into the lesion site is more efficacious than intravitreal injection. Although it is considered that axons will grow towards the source of NTFs but not away and hence become trapped in the lesion site (Berry et al., 2008), this is not always the case. For example one such study that transplanted fibroblasts expressing NT-3 into the lesion site promoted axon regeneration without these axons becoming trapped in the graft (Grill et al., 1997).

4.4 Conclusion

In conclusion the differentiation protocol used failed to induce differentiation of DPSCs into neurons. DPSCs however were still shown to possess potential in CNS injury but in their undifferentiated form. DPSCs could promote RGC axon regeneration in both *in vitro* and *in vivo* models of CNS injury and secondly, were neuroprotective in the *in vivo* model.

Although regeneration was not as robust as other studies that use a combination of treatment strategies, DPSCs are a unique candidate for cellular therapy in CNS injury with the potential to become one part of a successful combinatorial therapy. By acting as a continuous source of NTFs with the capabilities for autologous transplantation, DPSCs can fill one of many important niches in what would be required to create a successful pro-regenerative therapy.

5 References

Abematsu, M., Tsujimura, K., Yamano, M., Saito, M., Kohno, K., Kohyama, J., Namihira, M., Komiya, S., Nakashima, K., 2010. Neurons derived from transplanted neural stem cells restore disrupted neuronal circuitry in a mouse model of spinal cord injury. The Journal of Clinical Investigation 120, 3255-3266.

Ahmed, Z., Kalinski, H., Berry, M., Almasieh, M., Ashush, H., Slager, N., Brafman, A., Spivak, I., Prasad, N., Mett, I., Shalom, E., Alpert, E., Di Polo, A., Feinstein, E., Logan, A., 2011. Ocular neuroprotection by siRNA targeting caspase-2. Cell Death & Disease 2.

Arthur, A., Rychkov, G., Shi, S., Koblar, S.A., Gronthos, S., 2008. Adult Human Dental Pulp Stem Cells Differentiate Toward Functionally Active Neurons Under Appropriate Environmental Cues. STEM CELLS 26, 1787-1795.

Bareyre, F.M., Kerschensteiner, M., Raineteau, O., Mettenleiter, T.C., Weinmann, O., Schwab, M.E., 2004. The injured spinal cord spontaneously forms a new intraspinal circuit in adult rats. Nat Neurosci 7, 269-277.

Basso, D.M., Beattie, M.S., Bresnahan, J.C., 1995. A Sensitive and Reliable Locomotor Rating-Scale for Open-Field Testing in Rats. Journal of Neurotrauma 12, 1-21.

Benowitz, L.I., Yin, Y., 2007. Combinatorial treatments for promoting axon regeneration in the CNS: Strategies for overcoming inhibitory signals and activating neurons' intrinsic growth state. Developmental Neurobiology 67, 1148-1165.

Berry, M., Ahmed, Z., Lorber, B., Douglas, M., Logan, A., 2008. Regeneration of axons in the visual system. Restorative Neurology and Neuroscience 26, 147-174.

Blesch, A., Tuszynski, M.H., 2009. Spinal cord injury: plasticity, regeneration and the challenge of translational drug development. Trends in neurosciences 32, 41-47.

Cafferty, W.B.J., McGee, A.W., Strittmatter, S.M., 2008. Axonal growth therapeutics: regeneration or sprouting or plasticity? Trends in neurosciences 31, 215-220.

Caroni, P., Schwab, M.E., 1988. Antibody against myelin associated inhibitor of neurite growth neutralizes nonpermissive substrate properties of CNS white matter. Neuron 1, 85-96.

Chai, Y., Jiang, X., Ito, Y., Bringas, P., Han, J., Rowitch, D.H., Soriano, P., McMahon, A.P., Sucov, H.M., 2000. Fate of the mammalian cranial neural crest during tooth and mandibular morphogenesis. Development 127, 1671-1679.

Cho, S.-R., Kim, Y.R., Kang, H.-S., Yim, S.H., Park, C.-i., Min, Y.H., Lee, B.H., Shin, J.C., Lim, J.-B., 2009. Functional Recovery After the Transplantation of Neurally Differentiated Mesenchymal Stem Cells Derived From Bone Barrow in a Rat Model of Spinal Cord Injury. Cell Transplantation 18, 1359-1368.

Coutts, M., Keirstead, H.S., 2008. Stem cells for the treatment of spinal cord injury. Experimental Neurology 209, 368-377.

Ernfors, P., Lee, K.-F., Jaenisch, R., 1994. Mice lacking brain-derived neurotrophic factor develop with sensory deficits. Nature 368, 147-150.

Fouad, K., Krajacic, A., Tetzlaff, W., 2011. Spinal cord injury and plasticity: Opportunities and challenges. Brain Research Bulletin 84, 337-342.

Ghajar, J., 2000. Traumatic brain injury. The Lancet 356, 923-929.

Grill, R., Murai, K., Blesch, A., Gage, F.H., Tuszynski, M.H., 1997. Cellular Delivery of Neurotrophin-3 Promotes Corticospinal Axonal Growth and Partial Functional Recovery after Spinal Cord Injury. The Journal of Neuroscience 17, 5560-5572.

Gronthos, S., Mankani, M., Brahim, J., Robey, P.G., Shi, S., 2000. Postnatal human dental pulp stem cells (DPSCs) in vitro and in vivo. Proceedings of the National Academy of Sciences 97, 13625-13630.

Gu, W., Zhang, F., Xue, Q., Ma, Z., Lu, P., Yu, B., 2010. Transplantation of bone marrow mesenchymal stem cells reduces lesion volume and induces axonal regrowth of injured spinal cord. Neuropathology 30, 205-217.

Guimaraes, E.T., Cruz, G.S., de Jesus, A.A., de Carvalho, A.F.L., Rogatto, S.R., Pereira, L.D., Ribeiro-Dos-Santos, R., Soares, M.B.P., 2011. Mesenchymal and embryonic characteristics of stem cells obtained from mouse dental pulp. Archives of Oral Biology 56, 1247-1255.

Harada, H., Kettunen, P.i., Jung, H.-S., Mustonen, T., Wang, Y.A., Thesleff, I., 1999. Localization of Putative Stem Cells in Dental Epithelium and Their Association with Notch and Fgf Signaling. The Journal of Cell Biology 147, 105-120.

Huang, A.H.-C., Snyder, B.R., Cheng, P.-H., Chan, A.W.S., 2008. Putative Dental Pulp-Derived Stem/Stromal Cells Promote Proliferation and Differentiation of Endogenous Neural Cells in the Hippocampus of Mice. STEM CELLS 26, 2654-2663.

Huang, E.J., Reichardt, L.F., 2001. NEUROTROPHINS: Roles in Neuronal Development and Function1. Annual Review of Neuroscience 24, 677-736.

Huang, X., Saint-Jeannet, J.-P., 2004. Induction of the neural crest and the opportunities of life on the edge. Developmental Biology 275, 1-11.

Johnson, T.V., Bull, N.D., Hunt, D.P., Marina, N., Tomarev, S.I., Martin, K.R., 2010. Neuroprotective Effects of Intravitreal Mesenchymal Stem Cell Transplantation in Experimental Glaucoma. Investigative Ophthalmology & Visual Science 51, 2051-2059.

Kiraly, M., Kadar, K., Horvathy, D.B., Nardai, P., Racz, G.Z., Lacza, Z., Varga, G., Gerber, G., 2011. Integration of neuronally predifferentiated human dental pulp stem cells into rat brain in vivo. Neurochemistry International 59, 371-381.

Kiraly, M., Porcsalmy, B., Pataki, A., Kadar, K., Jelitai, M., Molnar, B., Hermann, P., Gera, I., Grimm, W.D., Ganss, B., Zsembery, A., Varga, G., 2009. Simultaneous PKC and cAMP activation induces differentiation of human dental pulp stem cells into functionally active neurons. Neurochemistry International 55, 323-332.

Kurimoto, T., Yin, Y.Q., Omura, K., Gilbert, H.Y., Kim, D., Cen, L.P., Moko, L., Kugler, S., Benowitz, L.I., 2010. Long-Distance Axon Regeneration in the Mature Optic Nerve: Contributions of Oncomodulin, cAMP, and pten Gene Deletion. Journal of Neuroscience 30, 15654-15663.

Leong, W.K., Henshall, T.L., Arthur, A., Kremer, K.L., Lewis, M.D., Helps, S.C., Field, J., Hamilton-Bruce, M.A., Warming, S., Manavis, J., Vink, R., Gronthos, S., Koblar, S.A., 2012. Human Adult Dental Pulp Stem Cells Enhance Poststroke Functional Recovery Through Non-Neural Replacement Mechanisms. Stem Cells Translational Medicine 1, 177-187.

Liu, K., Tedeschi, A., Park, K.K., He, Z.G., 2011. Neuronal Intrinsic Mechanisms of Axon Regeneration. Annual Review of Neuroscience, Vol 34 34, 131-152.

Logan, A., Ahmed, Z., Baird, A., Gonzalez, A.M., Berry, M., 2006. Neurotrophic factor synergy is required for neuronal survival and disinhibited axon regeneration after CNS injury. Brain 129, 490-502.

Miura, M., Gronthos, S., Zhao, M.R., Lu, B., Fisher, L.W., Robey, P.G., Shi, S.T., 2003. SHED: Stem cells from human exfoliated deciduous teeth. Proceedings of the National Academy of Sciences of the United States of America 100, 5807-5812.

Moon, L., Bunge, M.B., 2005. From Animal Models to Humans: Strategies for Promoting CNS Axon Regeneration and Recovery of Limb Function after Spinal Cord Injury. Journal of Neurologic Physical Therapy 29, 55-69 10.1097/1001.NPT.0000282512.0000216964.0000282594.

Nombela-Arrieta, C., Ritz, J., Silberstein, L.E., 2011. The elusive nature and function of mesenchymal stem cells. Nature Reviews Molecular Cell Biology 12, 126-131.

Nosrat, I.V., Widenfalk, J., Olson, L., Nosrat, C.A., 2001. Dental Pulp Cells Produce Neurotrophic Factors, Interact with Trigeminal Neurons in Vitro, and Rescue Motoneurons after Spinal Cord Injury. Developmental Biology 238, 120-132.

Papaccio, G., Graziano, A., d'Aquino, R., Graziano, M.F., Pirozzi, G., Menditti, D., De Rosa, A., Carinci, F., Laino, G., 2006. Long-term cryopreservation of dental pulp stem cells (SBP-DPSCs) and their differentiated osteoblasts: A cell source for tissue repair. Journal of Cellular Physiology 208, 319-325.

Park, K.K., Liu, K., Hu, Y., Smith, P.D., Wang, C., Cai, B., Xu, B., Connolly, L., Kramvis, I., Sahin, M., He, Z., 2008. Promoting Axon Regeneration in the Adult CNS by Modulation of the PTEN/mTOR Pathway. Science 322, 963-966.

Richardson, P.M., McGuinness, U.M., Aguayo, A.J., 1980. Axons from CNS neurones regenerate into PNS grafts. Nature 284, 264-265.

Sakai, K., Yamamoto, A., Matsubara, K., Nakamura, S., Naruse, M., Yamagata, M., Sakamoto, K., Tauchi, R., Wakao, N., Imagama, S., Hibi, H., Kadomatsu, K., Ishiguro, N., Ueda, M., 2012. Human dental pulp-derived stem cells promote locomotor recovery after complete transection of the rat spinal cord by multiple neuro-regenerative mechanisms. Journal of Clinical Investigation 122, 80-90.

Schwab, M., Caroni, P., 1988. Oligodendrocytes and CNS myelin are nonpermissive substrates for neurite growth and fibroblast spreading in vitro. The Journal of Neuroscience 8, 2381-2393.

Stone, E.M., Fingert, J.H., Alward, W.L.M., Nguyen, T.D., Polansky, J.R., Sunden, S.L.F., Nishimura, D., Clark, A.F., Nystuen, A., Nichols, B.E., Mackey, D.A., Ritch, R., Kalenak, J.W., Craven, E.R., Sheffield, V.C., 1997. Identification of a Gene That Causes Primary Open Angle Glaucoma. Science 275, 668-670.

Thomas, K.E., Moon, L.D.F., 2011. Will stem cell therapies be safe and effective for treating spinal cord injuries? British Medical Bulletin 98, 127-142.

Yu, J.H., He, H.X., Tang, C.B., Zhang, G.D., Li, Y.F., Wang, R.N., Shi, J.N., Jin, Y., 2010. Differentiation potential of STRO-1(+) dental pulp stem cells changes during cell passaging. Bmc Cell Biology 11.

A thesis submitted to the University of Birmingham in partial fulfilment of the requirements for the degree of

MASTER OF RESEARCH

Neurotrauma and Neurodegeneration

School of Clinical and Experimental Medicine

University of Birmingham

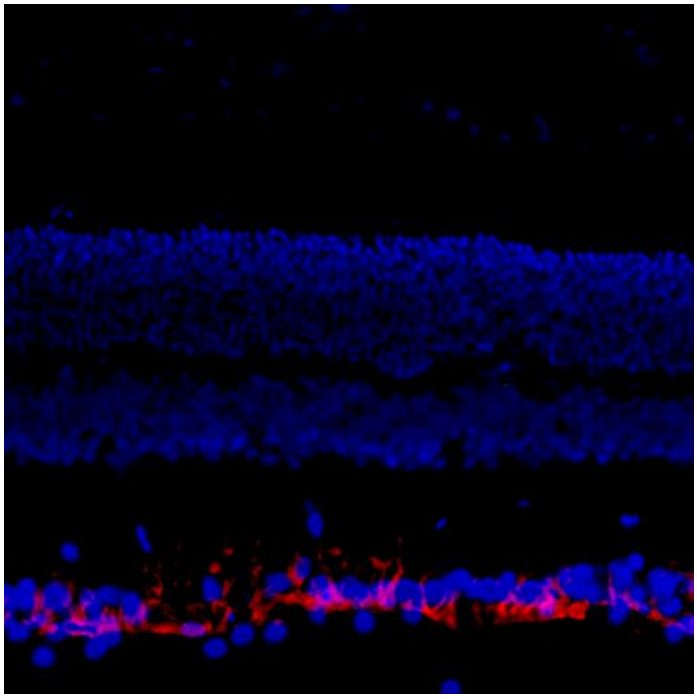

Establishing a rat model of proliferative vitreoretinopathy to evaluate Decorin as a potential treatment

Ben Mead

Supervisors: Prof Rob Scott, Prof Ann Logan and Maj Richard Blanch

Acknowledgements

I would first like to thank my supervisors Prof Rob Scott, Prof Ann Logan and Maj Richard Blanch for their support and guidance throughout the whole project. I would also like to thank Sarina Kundi for technical help with Western blotting. Finally, I would like to thank everyone in the Molecular Neuroscience Group for the friendly, welcoming atmosphere and providing help whenever needed.

Contents

List of figures

Abstract

Proliferative vitreoretinopathy (PVR), a sight threatening disease, is the major complication in the surgical treatment of retinal detachment. It is associated with intraocular fibrosis in the eye, often manifesting as membranes layering on top of, or underneath, the retina. These abnormal membranes can lead to further retinal detachments *via* myofibroblast-induced traction, ultimately causing blindness.

The aim of the present study was to develop a rat model of PVR by dual-intravitreal injection of transforming growth factor-β_2 (TGF-β_2) and fibroblast growth factor-2 (FGF-2) - with or without a retinal detachment induced by subretinal hyaluronate injection. Decorin, an anti-fibrotic agent, was tested for therapeutic efficacy at preventing PVR in the proposed model.

Immunohistochemistry was inappropriate for quantifying changes in the expression of specific fibrotic proteins. Western blots, however, showed an elevation in both laminin and fibronectin levels after TGF-β_2/FGF-2 injection with levels of laminin reduced following treatment with Decorin. Retinal detachment induced elevations in laminin and fibronectin levels and, when combined with intravitreal TGF-β_2/FGF-2 injection, also induced elevations in α-smooth muscle actin$^+$ myofibroblasts.

This study demonstrates that retinal detachment combined with intravitreal TGF-β_2/FGF-2 injection is the best model to induce PVR and that Decorin is a promising anti-fibrotic treatment in this context.

1.2 Proliferative vitreoretinopathy – an overview

Proliferative vitreoretinopathy (PVR) is a sight threatening disease affecting the vitreous and retina. It is an exaggerated and deleterious ocular wound healing response and, as such, often occurs following ocular injuries such as rhegmatogenous retinal detachment (RRD). Although surgery to reattach the retina has become progressively more successful, PVR is still the most common complication and reason for surgical failure in RRD (reviewed in Pastor, 1998). The defining feature of PVR is the formation of fibrocellular membranes (Figure 2; (Charteris, 1995). These membranes can be seen subretinally, epiretinally and/or within the vitreous (Hiscott et al., 1999), applying traction on the retina which can induce retinal breaks at new or previously treated sites and induce tractional retinal detachment and ultimately blindness (Pastor, 1998).

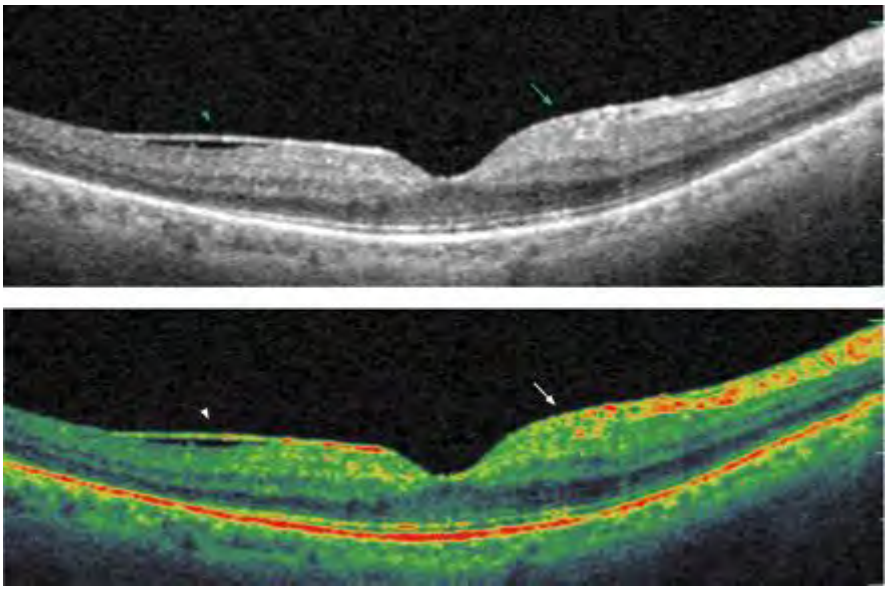

Figure 2: High-resolution spectral optical coherence tomography images in both grey-scale and colour of patients with proliferative vitreoretinopathy. Epiretinal membranes can be seen (arrows) that have formed on top of the retina (Brar et al., 2009).

1.3 Aetiology, current treatment and prognosis

PVR can occur in the context of many different ocular pathologies, such as RRD and trauma also a complication of their surgical treatments (Machemer, 1988). The incidence of PVR in patients with RRD ranges from 5-11% whereas in patients with more serious conditions such as giant retinal tears,

16-41% go on to develop PVR. Penetrating ocular trauma leads to PVR in 10-45% of patients (reviewed in Charteris et al., 2002).

Currently the only treatment for PVR is a surgical approach. Like RRD, detached retina is the primary pathology in PVR and so closure of any retinal breaks and retinal reattachment is the goal for the surgeon. For mild PVR, external scleral buckling remains a relatively non-invasive and successful technique (Charteris, 1995). For more severe cases of PVR, removal of epiretinal and subretinal membranes is necessary to treat the tractional forces they apply on the retina. Cryotherapy or laser photocoagulation may also be needed to induce adherence of regions of the broken retina to the choroid through the scarring response. Finally an intraocular tamponade such as silicone oil or the gas fluoropropane is used to help with retinal reattachment (Charteris, 1995).

Despite the Silicone study reporting an anatomical success rate of 77-79% (Charteris et al., 2002), patient's visual outcome remains poor and, as such, has led many to question whether surgery for PVR is justifiable (Mccormack et al., 1994). In the Silicone study, only 25% of post-operative PVR patients achieved a vision of 10/100 or greater (Charteris et al., 2002). Despite this over half of post-operative PVR patients did not regret having the surgery with just under half of patients saying the surgery was of some benefit to their vision (Mccormack et al., 1994).

1.4 Pathogenesis

PVR is an exaggerated form of wound healing after vitreoretinal injury and experimental evidence reveals three phases in its pathogenesis, similar to the three phases of a normal wound healing response (Pastor, 1998). This process, based on clinical findings, takes approximately 1-2 months (Pastor et al., 2002) and it is likely that the phases overlap significantly.

1.4.1 Phase I - Inflammation

Inflammation is a cascade of events after injury which aims to eliminate any remaining pathogens, clear damaged tissue and initiate the endogenous wound healing process (Gilbert et al., 1988). It starts with the initial injury itself, due to the breakdown of the blood-ocular barrier and the invasion of platelets into the lesion site. These platelets initiate an inflammatory cascade by recruiting inflammatory cells such as macrophages into the lesion site, although other sources of macrophages such as hyalocytes and retinal microglia have also been suggested to be involved (Gilbert et al., 1988). This recruitment is regulated by growth factors/cytokines that the platelets secrete, such as transforming growth factor-β (TGF-β) and platelet derived growth factor (PDGF), whereas the macrophages entering the lesion site begin secreting many other factors including fibroblast growth factor (FGF). Studies on human vitreous show significantly increased levels of FGF, PDGF (Cassidy et al., 1998) and TGF-β_2 (Connor et al., 1989) in eyes with RRD that goes on to develop PVR.

Since larger retinal injuries are associated with a higher incidence of PVR (Charteris et al., 2002), it is possible that this is due to a more extensive breakdown in the blood-ocular barrier. Many other risk factors for PVR, such as vitreous haemorrhage and cryotherapy, are also associated with inflammation and breakdown of blood ocular barriers (Charteris, 1995; Mccormack et al., 1994). This, however, cannot be the only instigator of PVR since diseases such as uveitis coincide with blood-ocular barrier breakdown but are rarely associated with PVR (Pastor et al., 2002).

Another important cell playing a role in this condition is the retinal pigment epithelial (RPE) cell which rests on a basement membrane known at Bruch's membrane, found between the retina and choroid (Hiscott et al., 1999). Retinal injury, as well as possible imbalances in matrix metalloproteinases and their inhibitors (Hiscott et al., 1999), free these cells, which migrate out in response to endogenous growth factors in the subretinal space, such as PDGF (Pastor, 1998). These RPE cells have been shown to differentiate into macrophages, complementing those in the inflammatory response, and also fibrocyte-like cells, complementing the scar formation of the

second phase (Machemer, 1988). It is suggested that this response by RPE cells is due, in part, to the loss of contact with their neighbouring photoreceptors in the retina (Agrawal et al., 2007).

1.4.2 Phase II - Proliferation and scar formation

FGFs, derived mostly from macrophages, stimulates the proliferation of fibroblasts, the cells responsible for the production of the extracellular matrix (ECM) and the formation of epiretinal membranes (Pastor, 1998). Although the origin of the fibroblasts is not fully known, RPE cells and astrocytes are two likely sources (Pastor et al., 2002). RPE cells undergo a special type of dedifferentiation known as epithelial-mesenchymal transition (EMT) whereby cells lose their epithelial morphology, taking on a more mesenchymal morphology and protein expression pattern (Pastor et al., 2002). These resulting myofibroblasts are positive for α-smooth muscle actin (α-SMA) and contribute to scar formation and contraction in PVR (Pastor et al., 2002).

PDGF, as well as potentiating the migration of RPE cells, stimulates their proliferation causing RPE cells to become a large component of epiretinal membranes. This stimulation occurs in an autocrine fashion as RPE cells themselves have been shown to produce PDGF (Cassidy et al., 1998). The interaction of RPE cells with epiretinal membranes is likely to be through their β_1 integrin receptors which usually anchor the cells to Bruch's membrane by binding to the laminin and collagen membrane components (Hiscott et al., 1999).

Glial cells, such as astrocytes and Müller cells, undergo astrogliosis in response to many types of neuronal injury (Berry et al., 2008; Pastor et al., 2002) which results in an astrogliotic scar. This scar, usually dedicated to walling off the injured neuronal tissue (reviewed in Rolls et al., 2009), is produced, to some degree, in PVR were it contributes to the pathology. These glial cells are derived from the retina and migrate out to proliferate on available membrane surfaces, forming another large component of epiretinal membranes (Machemer, 1988). Despite their importance in other

parts of the nervous system, their role in repairing the injured retina is not understood (Pastor et al., 2002).

Macrophages form another integral part of epiretinal membranes, being identified in 84-100% of epiretinal membrane samples from patients, in both acute and chronic (over 4 months old) epiretinal membranes (Gilbert et al., 1988). As well as contributing significantly to the cellular portion of epiretinal membranes, macrophages are involved in the formation of scar tissue.

1.4.3 Phase III - Scar modulation and epiretinal membrane contraction

Fibronectin and fibrin, originating from the serum following injury and ocular-blood barrier breakdown, forms a temporary ECM in the early phase of the wound healing response, concurrent with the initiation of inflammation. Later in the process, TGF-β orchestrates the deposition of a more permanent scar comprised of RPE cell-derived fibronectin, laminin and collagens (Connor et al., 1989; Hiscott et al., 1999; Pastor et al., 2002). Macrophages are also responsible for fibronectin deposition in both acute and chronic epiretinal membranes (Gilbert et al., 1988). Overall, ECM and epiretinal membranes have been shown to contain collagen I, III, IV, V, laminin, fibronectin and tenascin (Hiscott et al., 1999; Pastor, 1998; Pastor et al., 2002). Collagen II is also found in epiretinal membranes, although it is also found in healthy vitreous, thus it is unknown if it is truly upregulated or just captured from the surrounding tissue (Hiscott et al., 1999). Myofibroblasts, positive for α-SMA within the PVR scar tissue, apply tractional force to the retina and are ultimately responsible for repeated or new retinal redetachment (Kita et al., 2008; Pastor et al., 2002).

As the scar matures and its collagen density increases, the cellular components are removed *via* necrosis and phagocytosis of degenerate cellular material, possibly due to the increasingly fibrotic environment being deleterious to the cells (Hiscott et al., 1999). Visual loss is the end result of retinal detachment and studies seem to agree that the mechanism is photoreceptor apoptosis (Cook et al., 1995). This apoptotic response is possibly due trophic deprivation and separation from the

RPE. Other responses by photoreceptors to retinal detachment termed “remodelling” - include the redistribution of opsin proteins to the cell body and increased neurite extension (Charteris et al., 2002).

1.5 Animal models and experimental treatments

Although surgery remains the only routine treatment for PVR, various therapeutic agents have been designed and tested in clinical trials, which specifically target the cellular and molecular components involved in the three phases of scarring detailed above and believed to be critical to the pathology of PVR. To test these agents, over 25 animal models have been developed, all which attempt to recapitulate the pathogenesis of PVR (Agrawal et al., 2007).

The injection of cells into the vitreous is one category of PVR models. These models rely on injection of cells known to proliferate in the vitreous of PVR patients and contributing to epiretinal membranes, including fibroblasts, RPE cells and activated macrophages. Regardless of which cell is injected, the resultant epiretinal membranes often comprise multiple different cells that are seen in the human condition. Other models inject growth factors/cytokines, or cells that transgenically express growth factors known to be important in PVR, such as PDGF. Finally, other models mimic the initial insult by, (1) surgically damaging the retina to release RPE cells, (2), injecting hyaluronate subretinally to detach the retina or, (3), injecting autologous blood to mimic trauma (Agrawal et al., 2007).

Anti-proliferative agents which target the cell proliferation phase during the pathogenesis of PVR have been tested in clinical trials. Two of these compounds are 5-fluorouracil and daunomycin which, although well tolerated by the eye, produced minimal improvements in surgical success with no improved visual outcome (Charteris, 1995; Charteris et al., 2002). Another anti-proliferative agent tested is retinoic acid which inhibits RPE proliferation and differentiation. It appears that, following retinal detachment, RPE cells are no longer in the presence of retina-derived retinoic acid

so they undergo proliferation and differentiation (Charteris, 1995). A study administering retinoic acid intravitreally *via* a slow release mechanism reported some success in an animal model of PVR (Giordano et al., 1993). Corticosteroids have also been implicated as a viable therapy both for their anti-inflammatory and anti-proliferative effects (Machemer, 1988).

The ECM, particularly that which makes up the epiretinal membranes and associated scar is another potential drug target. One drug that has been extensively studied is heparin which not only targets fibrin, responsible for the initial scar, but also binds and sequesters the activity of growth factors such as FGF and PDGF and thereby inhibits RPE cell proliferation. Although promising, heparin is also associated with an increased incidence of intraoperative bleeding (Charteris, 1995).

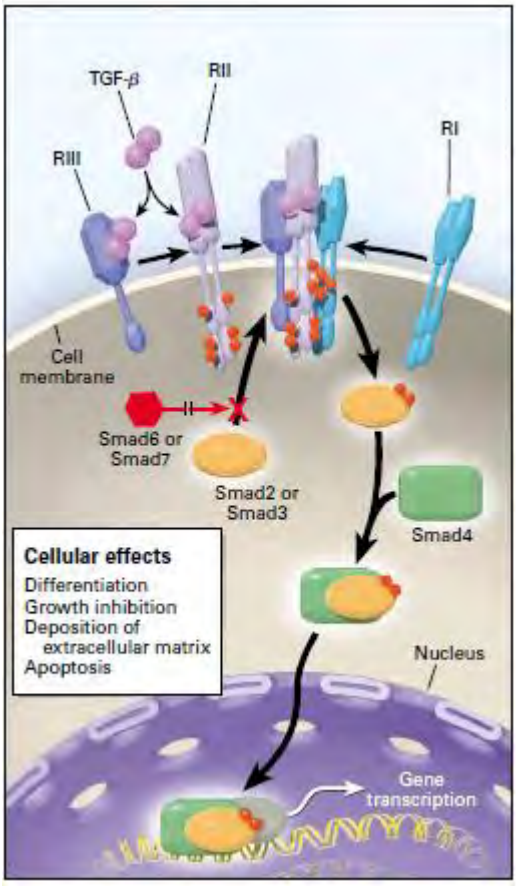

Figure 3: Transforming growth factor-β (TGF-β) signals through membrane bounds receptors known as RI, RII and RIII. TGF-β binds RIII which is presented to RI with the help of RII, leading to the phosphorylation of RI. TGF-β can also phosphorylate RI directly. Smads, intracellular transcription factors which make up the signalling pathway for TGF-β subsequently become activated. Smad2 or Smad3 become phosphorylated by RI which then complex with Smad4. This complex travels to the nucleus and through activation of gene transcription, induces the effects listed above. Two other Smads, Smad6 and Smad7 lack the ability to be activated by RI serving instead to only interfere with the signalling process. For this reason, Smad6 and Smad7 can be seen as inhibitors to the Smad signalling cascade (Blobe et al., 2000).

1.6 Fibrosis in proliferative vitreoretinopathy

Fibrosis is a critical step in the pathobiology of PVR. TGF-βs, a family of multifunctional cytokines which exist as three isomers in mammals termed TGF-β_1, TGF-β_2, and TGF-β_3, are pivotal in this process. Upon secretion, TGF-β is activated extracellularly before eliciting its cellular effects through a receptor complex and the Smad signalling pathway, depicted in Figure 3 (reviewed in Blobe et al., 2000). Other signalling pathways activated by TGF-β are continuously being uncovered;

one example being the RhoA pathway which is implicated in myofibroblast contraction (Derynck and Zhang, 2003; Kita et al., 2008).

As well as being elevated in the vitreous of patients with PVR (Connor et al., 1989), TGF-β increases the contraction of collagen fibres in an *in vitro* model of PVR (Pena et al., 1994). It is secreted by RPE cells, a dominant cell in epiretinal membranes. Injection of TGF-β and fibronectin into the vitreous of animals following a retinal injury induces intraocular fibrosis and tractional retinal detachment (Connor et al., 1989).

As mentioned previously, a cellular contributor to PVR fibrosis are myofibroblasts, which are derived from RPE cells through a specialised type of differentiation known as EMT. A study using experimental detachment of the retina in Smad3 knockout mice showed that the EMT of RPE cells is completely blocked, revealing that TGF-β signalling through the Smad pathway is critical for RPE cell EMT (Saika et al., 2004). The study then showed that without EMT, deposition of fibrous tissue and the formation of a retinal scar fails to occur in this trauma-induced mouse model of PVR. Smad7, an inhibitor of the TGF-β signalling pathway (Figure 3), can be overexpressed in cells *via* transfection which results in inhibition of the Smad pathway. When eyes from an animal model of PVR were transfected with Smad7, EMT and scar formation was inhibited (Saika et al., 2007).

As well as causing fibrosis, myofibroblasts contribute to the contraction of retinal membranes and the resulting tractional retinal detachment. Although TGF-β is implicated indirectly because it promotes EMT, it is also involved directly in epiretinal membrane contraction. This is because TGF-β activates other, Smad-independent signalling pathways, one of which is RhoA (Derynck and Zhang, 2003; Kita et al., 2008). The RhoA pathway is involved in contraction *via* the phosphorylation of myosin light chain (MLC). Contraction of collagen gels in response to vitreous samples from patients with PVR is strongly correlated with the concentration of activated TGF-β_2 (Kita et al., 2008). This MLC phosphorylation and resultant contractile response was inhibited by either antibodies to TGF-β or fasudil, a specific inhibitor of the RhoA pathway. Fasudil, when injected into the vitreous of

animals with experimental PVR, prevented tractional retinal detachment and thus preserved retinal cell viability.

1.7 Decorin, a potential treatment for PVR

The large role TGF-β plays in PVR combined with the observation that it is increased in PVR patients (Connor et al., 1989) has made TGF-β a potential therapeutic target for future treatments. Although antibodies against TGF-β exist, a natural inhibitor was discovered in 1990 (Yamaguchi et al., 1990), termed decorin. Decorin belongs to a group of molecules known as small leucine-rich proteoglycans and is found "decorating" collagen fibrils, thus contributing to collagen fibrillogenesis. Decorin plays a role in wound healing through facilitataly ECM remodelling, with one mechanism being the induction of matrix metalloproteinases (Iozzo, 1997). Decorin's ability to attenuate fibrosis through inhibition of TGF-β was shown to be effective at preventing the scarring associated with experimental kidney disease (Border et al., 1992) and penetrating brain injury (Logan et al., 1999). Other studies have highlighted an anti-fibrotic mechanism of decorin, independent of its ability to antagonize TGF-β (Fukui et al., 2001).

Decorin has been tested as a treatment for a variety of ocular disorders such as conjuctival scarring following glaucoma filtration surgery (Grisanti et al., 2005) and corneal scarring which often follows refractive laser surgery (Mohan et al., 2010), both studies giving promising results. Finally, Decorin has been shown to be effective after experimental retinal injury-induced PVR, significantly reducing tractional retinal detachment (Nassar et al., 2011). Unfortunately no detailed histopathological analysis was done.

1.8 Aims

The aim of this study was to develop a rat model of PVR using intravitreal injections of FGF-2 and TGF-β_2 combined with retinal detachment induced by subretinal injection of Healon. Decorin, a TGF-β antagonist, was assessed as a potential treatment for PVR, both as a preventive therapy, given during the development of PVR and as a curative therapy, given following the establishment of PVR.

1.9 Hypothesis

Intravitreal TGF-β_2 and FGF-2 induces PVR in rats placing their presence in patients with PVR as potentially causative. Decorin, a known inhibitor of TGF-β with anti-fibrotic properties prevents PVR or, if given after PVR is established, ameliorates the fibrosis associated with the disease.

2 Material and methods

2.1 Reagents

All reagents in this project were provided by Sigma (Poole, UK) unless otherwise stated. TGF-β_2 (Peprotech, London, UK) was supplied and intravitreally injected at a concentration of 5µg/ml. It was injected in a volume of 3.5µl which, assuming the vitreous volume of an adult rat is approximately 50µl (Berkowitz et al., 1998), would produce a working concentration of approximately 350ng/ml. FGF-2 (Abcam, Cambridge, UK) was supplied at a concentration of 50µg/ml and diluted to 1µg/ml in sterile PBS. It was injected in a volume of 2.5µl to produce a working concentration of 50ng/ml which is within its active range (Logan et al., 2006). Decorin (Galacorin™; Catalent Pharma Solutions, Middleton, UK) was used at a concentration of 5mg/ml in PBS and injected in a volume of 4µl to produce a working concentration of approximately 400µg/ml in the rat vitreous. This is an effective concentration since other studies using 2kg rabbits have injected 100-200µg of Decorin which, based on the rabbit vitreous volume being approximately 0.5ml/kg body weight (Shafiee et al., 2008), would produce a working concentration of 100-200µg/ml. Healon 0.25% was made up from Healon 2.3% (Abbot Medical Optics, California, USA) diluted in sterile PBS. Antibodies used were from Sigma, Abcam (Cambridge, UK), Serotec (Oxford, UK), Molecular Probes (Leiden, Netherlands) and GE Healthcare (Buckinghamshire, UK) (Table 2).

2.2 Experimental design

The experiment was designed to test the induction and attenuation of PVR in the rat after 28 days and utilized 4 animal groups, each group comprised of 4 animals (Table 1).

Animal Group 1 (n=4)		Animal Group 2 (n=4)	
Left eye	**Right eye**	**Left eye**	**Right eye**
Retinal detachment (Day 0) + *ivit* injection of PBS (Day 0 and 2)	Retinal detachment (Day 0) + *ivit* injection of TGF-β_2 and FGF-2 (Day 0 and 2)	*Ivit* injection of PBS(Day 0 and 2)	*Ivit* injection of TGF-β_2 and FGF-2 (Day 0 and 2)
Animal Group 3 (n=4)		**Animal Group 4 (n=4)**	
Bi-weekly PBS injection (beginning day 14)	**Bi-weekly Decorin injections (beginning day 14)**	**Bi-weekly PBS injection**	**Bi-weekly Decorin injections**
Left eye	**Right eye**	**Left eye**	**Right eye**
Ivit injection of TGF-β_2 and FGF-2 (Day 0 and 2)	*Ivit* injection of TGF-β_2 and FGF-2 (Day 0 and 2)	*Ivit* injection of TGF-β_2 and FGF-2 (Day 0 and 2)	*Ivit* injection of TGF-β_2 and FGF-2 (Day 0 and 2)

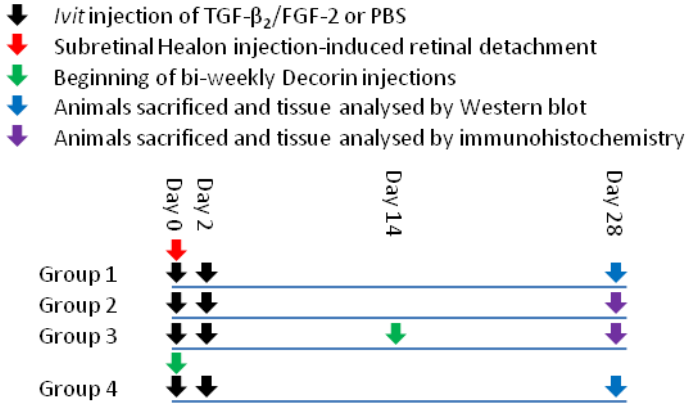

Table 1: The experimental design is given above including a table of the 4 animal groups with the treatments they received and a timeline of the study. All animals received a retinal injury by trans-scleral needle puncture. Animal groups 1 and 2 are aimed at creating the rat model of proliferative vitreoretinopathy (PVR). Group 1 received, in the right eye, subretinal Healon (day 0) with intravitreal (*ivit)* injection of transforming growth factor-β_2 (TGF-β_2) and fibroblast growth factor-2 (FGF-2) on both day 0 and day 2. The left eye served as the control, with growth factors replaced by phosphate-buffered saline (PBS) of an equal volume. Group 2 was the same as group 1 but with subretinal Healon omitted. Group 4 was the same as group 2 however they also received bi-weekly injections of Decorin in the right eye to assess its potential as a therapy for treating PVR. To control for the Decorin, the left eye received bi-weekly PBS injections instead of Decorin. Group 3 was the same as group 4 except bi-weekly injections of Decorin/PBS were delayed by 2 weeks to assess its ability to reverse an already established scar. All animals were sacrificed on day 28. Western blots were performed on group 1 and 4 while immunohistochemistry was done on group 2 and 3.

2.3 Animals

Sixteen female Lister-Hooded rats weighing 170-200g were used for this experiment. All surgical procedures were carried out under Home Office guidelines in accordance with animal act 1986 (UK) and after local ethical approval (BERSC). Animals were kept in a temperature and humidity controlled environment (21°, 55% humidity). Animals were given food/water *ad libitum* and kept under a 12 hour light and dark cycle with a daytime luminance of 80lux. For anaesthetic induction, 5% Isoflurane/1.5L per minute O_2 was used with isoflurane being lowered to 3.5% prior to surgery. The pedal reflex was used to assess animal sedation prior to surgery.

2.4 Intravitreal injections

Isoflurane administration was maintained at 3.5% throughout the surgery. The head was rotated 45° so the eye to be injected was in the superior position. Using angled non-toothed forceps, the eye was gently prolapsed from the socket up to the point where the limbus was seen. A sterile cotton bud pressed posterior to the eye aided in prolapsing it. Forceps were tightened gently around the eye to keep it rigid without compromising its blood supply. A glass micropipette produced from pulled glass capillary rods (Harvard apparatus, Edenbridge, Kent, UK) using a Flaming-Brown micropipette puller (Sutter instruments, California, USA) was preloaded with TGF-β_2 and FGF-2, PBS or Decorin solution, ready for injection. Intravitreal Injections with the loaded micropipettes were done at the angle shown in Figure 4 at the temporal side of the eye and, to relieve ocular pressure, the eye was penetrated trans-sclerally with a 23G needle tip at a point 180° from the original injection site (nasally), which also created a retinal injury. For retinal detachment in animal group 1, 5 - 10µl of 0.25% Healon (Abbot Medical Optics, Santa Ana, California, USA) in PBS was injected into the subretinal space.

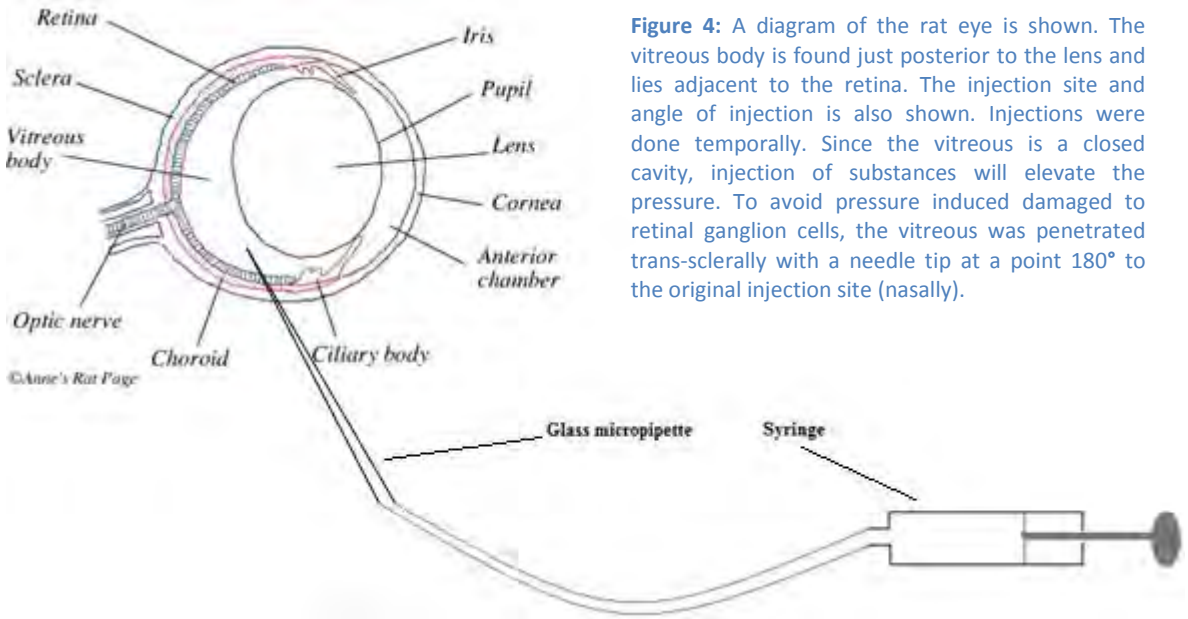

Figure 4: A diagram of the rat eye is shown. The vitreous body is found just posterior to the lens and lies adjacent to the retina. The injection site and angle of injection is also shown. Injections were done temporally. Since the vitreous is a closed cavity, injection of substances will elevate the pressure. To avoid pressure induced damaged to retinal ganglion cells, the vitreous was penetrated trans-sclerally with a needle tip at a point 180° to the original injection site (nasally).

2.5 Tissue preparation – immunofluorescence

At the end of the study (day 28), animals from groups 2 and 3 were intraperitoneally injected with 0.5ml Ketamine + Medetomidine. After 15 minutes, 4% paraformaldehyde (PFA; TAAB, Reading, UK) in PBS was used for intracardiac perfusion with concurrent clamping of the descending aorta to limit fixation to the head region. Eyes were dissected out by cutting around the orbit and separating the eye from the extraocular muscles and optic nerve. The cornea and lens of the eyes were dissected away leaving a retinal cup which was imaged on a dissecting microscope, before being post-fixed in 4% PFA in PBS for 24 hours at 4°C. The tissue was then cryoprotected in 10%, 20% and 30% sucrose solution in PBS for 24 hours, each at 4°C. Eyes were then embedded using optimal cutting temperature (OCT) embedding medium (Thermo Shandon, Runcorn, UK) in peel-away mould containers (Agar Scientific, Stansted, Essex, UK) which were kept under crushed dry ice for 5-10 minutes to allow the OCT to freeze. Frozen tissue blocks were stored at -20°C to be sectioned.

Following embedding, eyes were sectioned on a cryostat microtome (Bright, Huntingdon, UK) maintained at -22°C and at a thickness of 15µm before being mounted on positively charged glass slides (Superfrost Plus, Fisher Scientific, Pittsburgh, USA). Slides were left to dry overnight at 37°C before being stored at -20°C.

2.6 Tissue preparation – Western blot

At the end of the study (day 28), animals from groups 1 and 4 plus intact animals were sacrificed by intraperitoneal injection of Euthanal (sodium pentobarbital). The eyes were removed and retinae dissected out and snap frozen in liquid nitrogen. The tissue was defrosted on ice, and homogenized for 1 minute in cold lysis buffer (150mM NaCl, 20mM Tris HCl (Fisher BioReagents, UK), 1mM EDTA (Fisher BioReagents), 0.5mM EGTA, 1% NP-40 and 5µl/ml protease inhibitor cocktail). The homogenized tissue was left on ice for 20 minutes before being centrifuged at 16,000 xg for 30

minutes at 4°C. The supernatant was collected and the protein concentration determined using the colorimetric DC protein assay (BioRad, Hercules, CA, USA) as per the manufacturer's instructions.

2.7 Western blot

Samples (40µg total protein) were made up to 20ml in 2x Laemmli loading buffer and incubated for 4 minutes at 90°C. Samples were loaded and separated on an 8% SDS-polyacrylamide gel (Life Technologies, Invitrogen, UK) while in running buffer (192mM glycine, 25mM Tris base, 0.1% SDS (Fisher BioReagents)) for 2 hours. PVDF membranes (Millipore, Gloucestershire, UK) were activated in methanol for 1 minute and then washed in transfer buffer (192mM glycine, 25mM Tris base, 20% methanol, 0.01% SDS). Proteins were transferred to the PVDF membranes in transfer buffer before being washed in TTBS (11.6mM Tris base, 38.1mM Tris HCl, 150mM NaCl, 0.05% Tween 20; pH 7.4). PVDF membranes were blocked for 1 hour in blocking solution (TTBS, 5% non-fat milk) and then incubated with the relevant primary antibody diluted in blocking solution for 2 hours at room temperature. Membranes were then washed for 3 X 10 minutes in TTBS before incubation with a HRP-conjugated secondary antibody for 1 hour at room temperature. Membranes were developed using an enhanced chemiluminescence system (Amersham, Buckinghamshire, UK). Blots were stripped using 2 X 10 minutes of stripping buffer (200mM glycine, 3.5mM SDS and 1% Tween 20), 2 X 10 minutes of PBS and 2 X 5 minutes TTBS before being reprobed with other relevant antibodies from thereafter.

2.8 Antibodies

Antigen specificity	Animal raised in	Dilution (immunofluorescence)	Dilution (Western blot)	Supplier
Laminin	Rabbit	1:200	1:250	Sigma
Fibronectin	Rabbit	N/A	1:500	Sigma
GFAP	Rabbit	1:250	N/A	Sigma
α-SMA	Mouse	1:100	1:1000	Sigma
β-actin	Mouse	N/A	1:1000	Sigma
ED1 (CD68)	Mouse	1:200	N/A	Serotec
Collagen IV	Rabbit	1:200	N/A	Abcam
Alexa-488 Mouse IgG	Goat	1:400	N/A	Molecular Probes
Alexa-594 Rabbit IgG	Goat	1:400	N/A	Molecular Probes
HRP-Mouse IgG	Sheep	N/A	1:1000	GE Healthcare
HRP-Rabbit IgG	Donkey	N/A	1:1000	GE Healthcare

Table 2: A list of antibodies used, animals they were raised in, dilution used for each technique (if applicable) and the supplier.

2.9 Immunohistochemistry

Frozen Sections were allowed to equilibrate to room temperature for 30 minutes before being hydrated in PBS for 2 X 5 minutes. Tissue was then permeabilized in 0.1% triton x-100 in PBS for 20 minutes at room temperature. Tissue was washed for 2 X 5 minutes in PBS and isolated with a hydrophobic PAP pen (Immedge pen; Vector Laboratories, Peterborough, UK). The tissue was blocked (75µl; 0.5% bovine serum albumin (g/ml), 0.3% Tween-20, 15% normal goat serum (Vector Laboratories) in PBS) in a humidified chamber for 30 minutes at room temperature. After the 30 minutes block, tissue was incubated with primary antibody diluted in antibody diluting buffer (ADB; 0.5% bovine serum albumin (g/ml), 0.3% Tween-20 in PBS) overnight at 4°C. The following day slides were left to equilibrate with room temperature for 20 minutes before being washed in 3 X 5 minutes of PBS. Tissue sections were then incubated with secondary antibody diluted in ADB for 1 hour in a hydrated incubation chamber at room temperature. After the 1 hour, slides were washed in 3 X 5 minutes of PBS, mounted in Vectorshield mounting medium containing DAPI (Vector Laboratories) and stored at 4°C prior to microscopic analysis.

2.10 Microscopy and analysis

Sections were analysed blind using a Zeiss Axioplan-2 fluorescent microscope (Carl Zeiss Ltd, Hertfordshire, UK) with images taken at 20X magnification using Axiocam HRc camera and Axiovision software (Carl Zeiss Ltd). Four sections per animal were used and 4 animals per treatment group with all sections used being in the same plane by ensuring the optic nerve was visible.

For Western blots, developed membranes were scanned onto computer and densitometry was performed on each band in the image using Photoshop CS3 (Adobe Systems inc, San Jose, CA, USA). This was done using a specific sized boxed drawn around the band and mean pixel intensity calculated and standardized to β-actin controls. Laminin bands were contrast enhanced on Photoshop CS3 to improve visibility.

2.11 Statistics

Densitometric data was standardised to β-actin controls first and then secondly to intact controls and thus given as normalised values.

3 Results

3.1 Overview

The study aimed to induce PVR in a rat and explore Decorin as a potential treatment option in ameliorating the fibrosis associated with the disease. A second aim of the study was to explore methods of quantifying retinal/vitreal fibrosis to determine the best technique. Group 1 was injected subretinally with Healon and then intravitreally with either PBS (left eye) or TGF-β_2/FGF-2 (right eye). Group 2 was injected intravitreally with either PBS (left eye) or TGF-β_2/FGF-2 (right eye). Group 3 was injected intravitreally with TGF-β_2/FGF-2 with delayed (day 14) intravitreal injection of either PBS (left eye) or Decorin (right eye). Group 4 was injected intravitreally with TGF-β_2/FGF-2 with intravitreal injection of either PBS (left eye) or Decorin (right eye). Groups 1 and 4 were analyzed using Western blot whereas groups 2 and 3 were analysed using immunohistochemistry.

3.2 Group 1

Subretinal injection of Healon increased fibronectin density in the retina at day 28 by over 2-fold (Figure 5A) and the laminin by more than 3-fold (Figure 5B). Injection of TGF-β_2/FGF-2 did not have any further effect on laminin/fibronectin density compared to PBS. Subretinal Healon injection with intravitreal TGF-β_2/FGF-2 increased α-SMA by 3-fold (Figure 5C) whereas without TGF-β_2/FGF-2, no effect compared to control was seen.

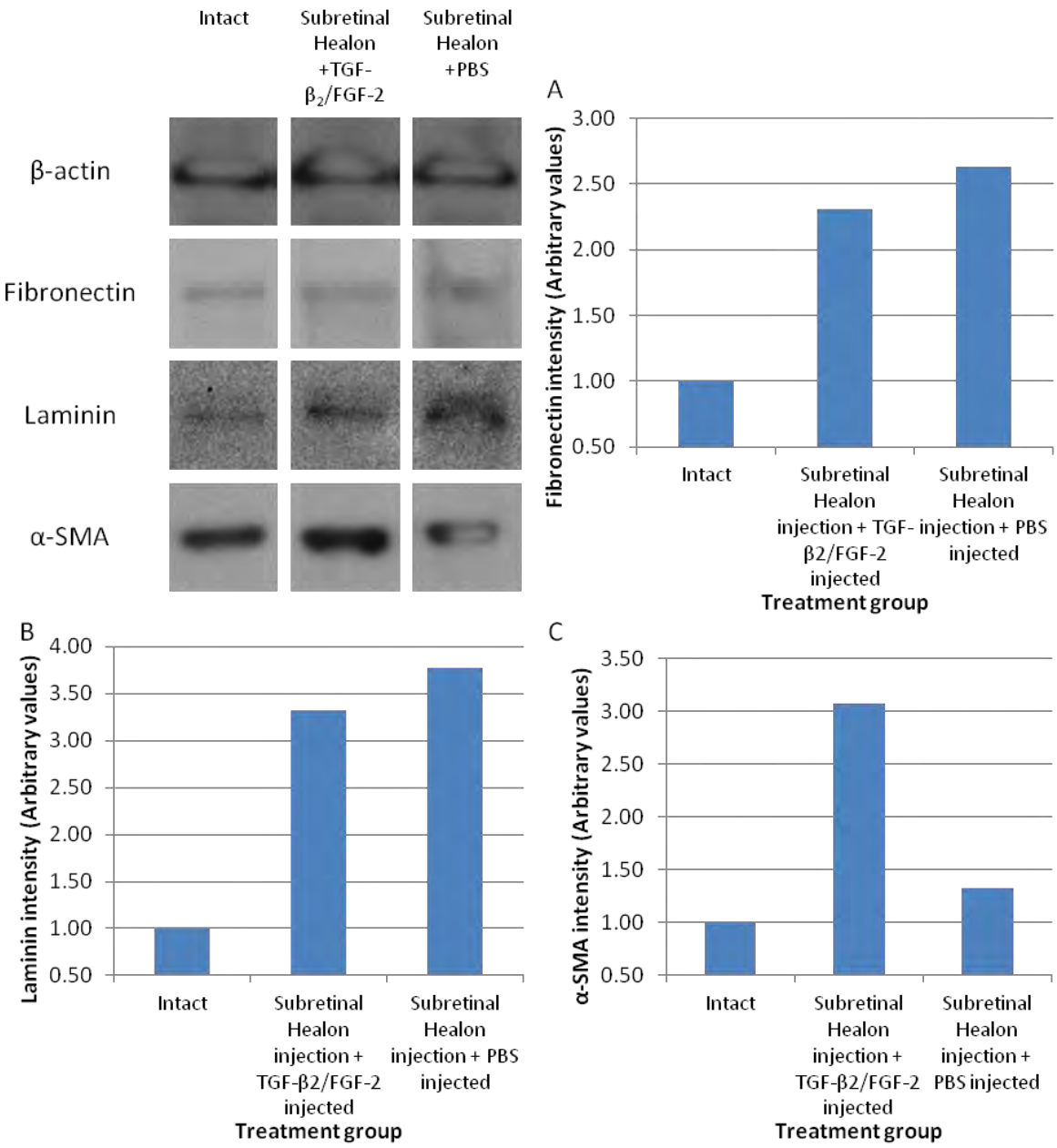

Figure 5: Western blots for animal group 1 that received a subretinal injection of Healon and intravitreal injection of either transforming growth factor-β_2/fibroblast growth factor-2 (TGF-β_2/FGF-2; right eye) or phosphate-buffered saline (PBS; left eye). Blots are shown above with densitometric data for fibronectin (A), laminin (B) and α-smooth muscle actin (α-SMA; C) displayed. Data is given as arbitrary values standardised to β-actin loading controls and then to intact eyes. Each treatment group consisted of 4 animals with samples pooled together before blotting.

3.3 Group 2

Gross macroscopic images of retinae from eyes intravitreally injected with PBS (left, Figure 6A) or TGF-β_2/FGF-2 (right, Figure 6B) yielded no signs of fibrosis and no discernible morphological difference at day 28. Small zones of haemorrhage (white arrows) could be visualised in both treatment groups. Immunohistochemically stained retinal sections showed GFAP (Figure 7A and B), laminin (Figure 7D and E) and collagen IV (Figure 7F and G) positive regions in the ganglion cell layer whereas ED1 (Figure 7A and B) and α-SMA (Figure 7D and E) was absent. No observable differences could be seen between treatment groups.

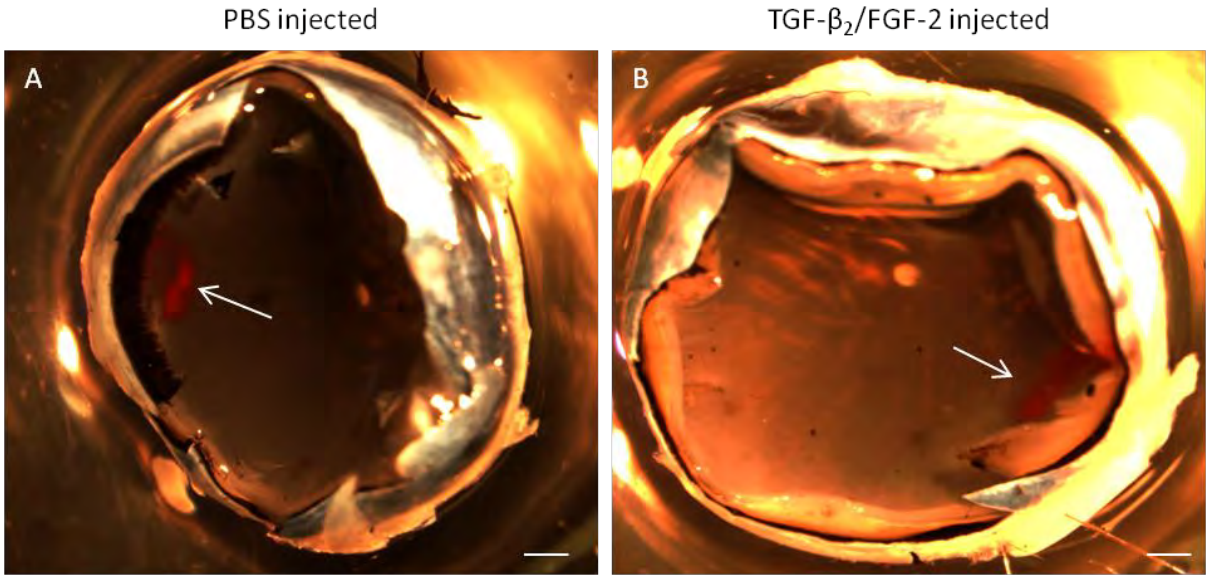

Figure 6: Gross macroscopic images of eyes from group 2 animals injected with either phosphate-buffered saline (PBS; left, A) or transforming growth factor-β_2/fibroblast growth factor-2 (TGF-β_2/FGF-2; right, B). White arrows point to areas of haemorrhage. Images were taken after removal of cornea and lens with multiple images at different exposures taken and merged into a high dynamic range image on Photoshop CS3. All images are representative of the 4 animals used. Scale bars = 1mm.

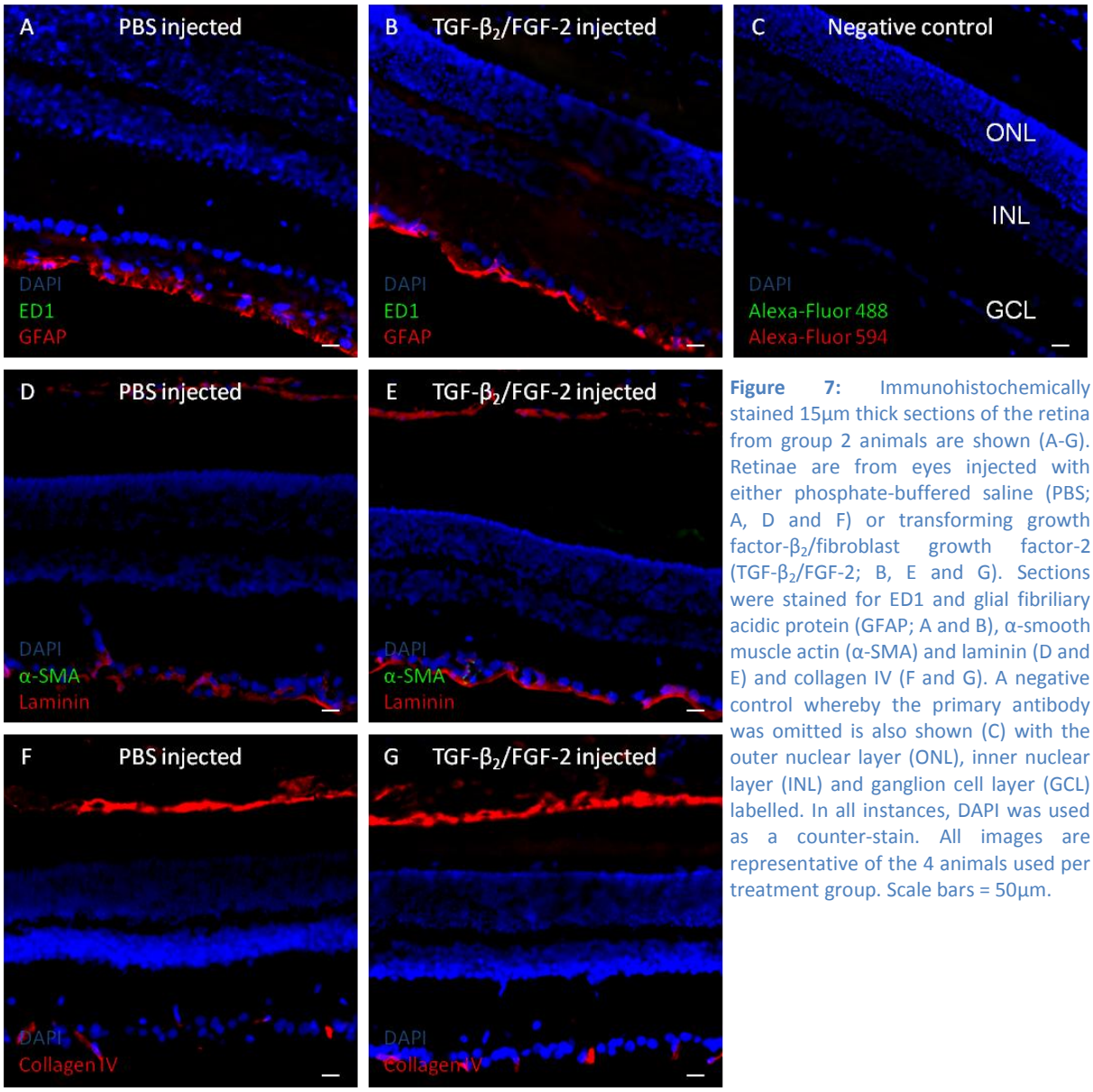

Figure 7: Immunohistochemically stained 15µm thick sections of the retina from group 2 animals are shown (A-G). Retinae are from eyes injected with either phosphate-buffered saline (PBS; A, D and F) or transforming growth factor-β_2/fibroblast growth factor-2 (TGF-β_2/FGF-2; B, E and G). Sections were stained for ED1 and glial fibriliary acidic protein (GFAP; A and B), α-smooth muscle actin (α-SMA) and laminin (D and E) and collagen IV (F and G). A negative control whereby the primary antibody was omitted is also shown (C) with the outer nuclear layer (ONL), inner nuclear layer (INL) and ganglion cell layer (GCL) labelled. In all instances, DAPI was used as a counter-stain. All images are representative of the 4 animals used per treatment group. Scale bars = 50µm.

3.4 Group 3

Gross macroscopic images of retinae from eyes intravitreally injected with TGF-β_2/FGF-2 and either PBS (left, Figure 8A) or Decorin (right, Figure 8B) yielded no signs of fibrosis and no discernible morphological difference at day 28. Immunohistochemically stained retinal sections showed GFAP (Figure 9A and B), laminin (Figure 9D and E) and collagen IV (Figure 9F and G) positive regions in the ganglion cell layer whereas ED1 (Figure 9A and B) and α-SMA (Figure 9D and E) was absent. No observable differences could be seen between treatment groups.

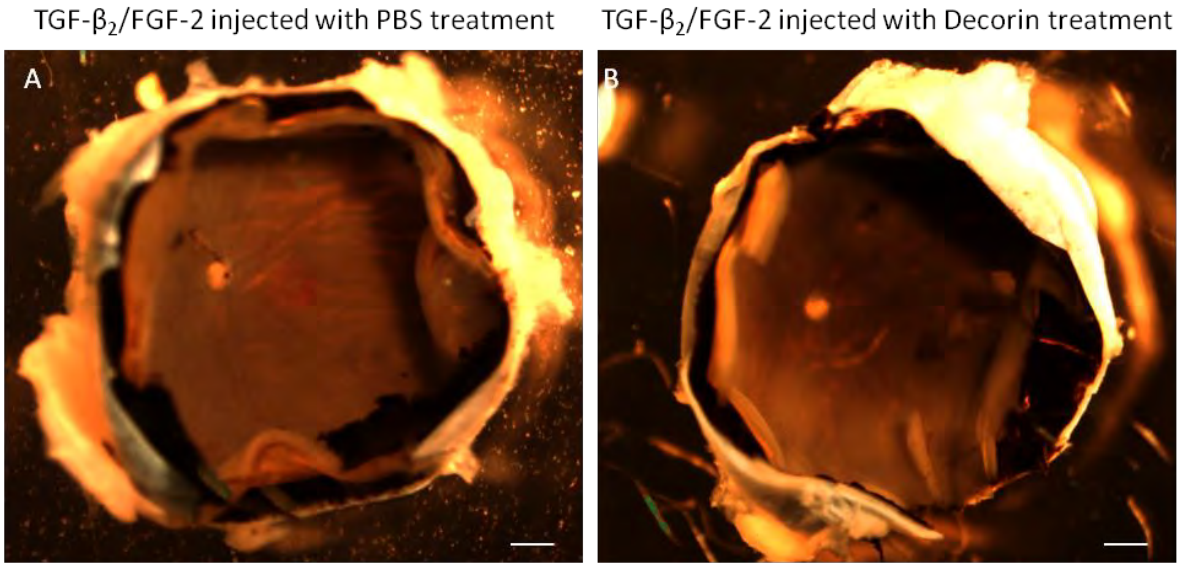

Figure 8: Gross macroscopic images of eyes from group 3 animals injected with transforming growth factor-β_2/fibroblast growth factor-2 (TGF-β_2/FGF-2) and treated at day 14 with either phosphate-buffered saline (PBS; left, A) or Decorin (right, B). Images were taken after removal of cornea and lens with multiple images at different exposures taken and merged into a high dynamic range image on Photoshop CS3. All images are representative of the 4 animals used. Scale bars = 1mm

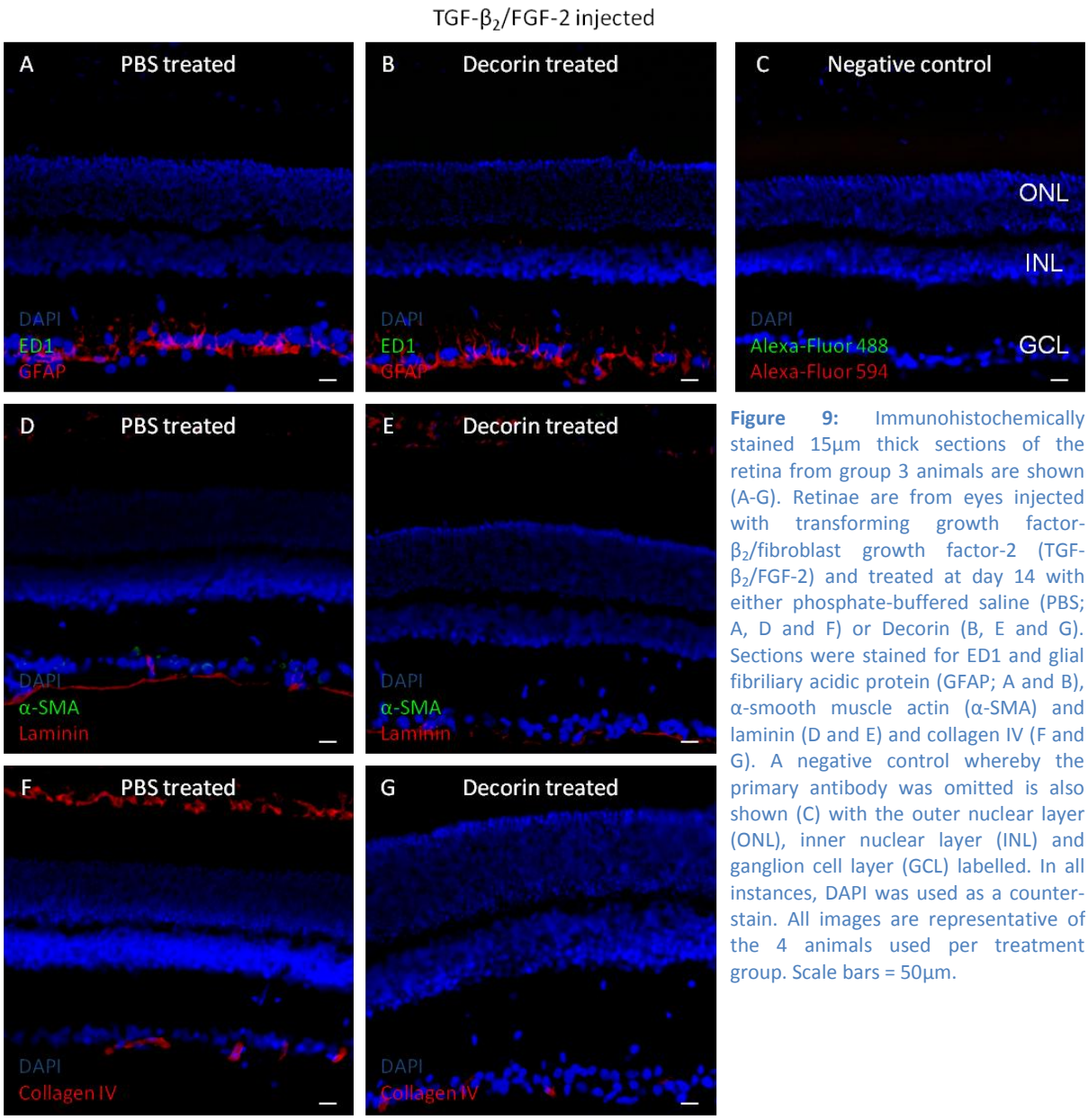

Figure 9: Immunohistochemically stained 15µm thick sections of the retina from group 3 animals are shown (A-G). Retinae are from eyes injected with transforming growth factor-β_2/fibroblast growth factor-2 (TGF-β_2/FGF-2) and treated at day 14 with either phosphate-buffered saline (PBS; A, D and F) or Decorin (B, E and G). Sections were stained for ED1 and glial fibriliary acidic protein (GFAP; A and B), α-smooth muscle actin (α-SMA) and laminin (D and E) and collagen IV (F and G). A negative control whereby the primary antibody was omitted is also shown (C) with the outer nuclear layer (ONL), inner nuclear layer (INL) and ganglion cell layer (GCL) labelled. In all instances, DAPI was used as a counter-stain. All images are representative of the 4 animals used per treatment group. Scale bars = 50µm.

3.5 Group 4

Intravitreal injection of TGF-β_2/FGF-2 (and PBS) increased fibronectin levels in the retina by over 2-fold (Figure 10A) and laminin levels by almost 5-fold (Figure 10B) compared to intact. Injection of Decorin alongside TGF-β_2/FGF-2 further increased fibronectin density, yielding a 3-fold elevation above intact. Laminin density, however, was reduced by half in the Decorin treated group. Intravitreal TGF-β_2/FGF-2 elicited a minor increase in α-SMA density (Figure 10C) that was seen with or without the presence of Decorin.

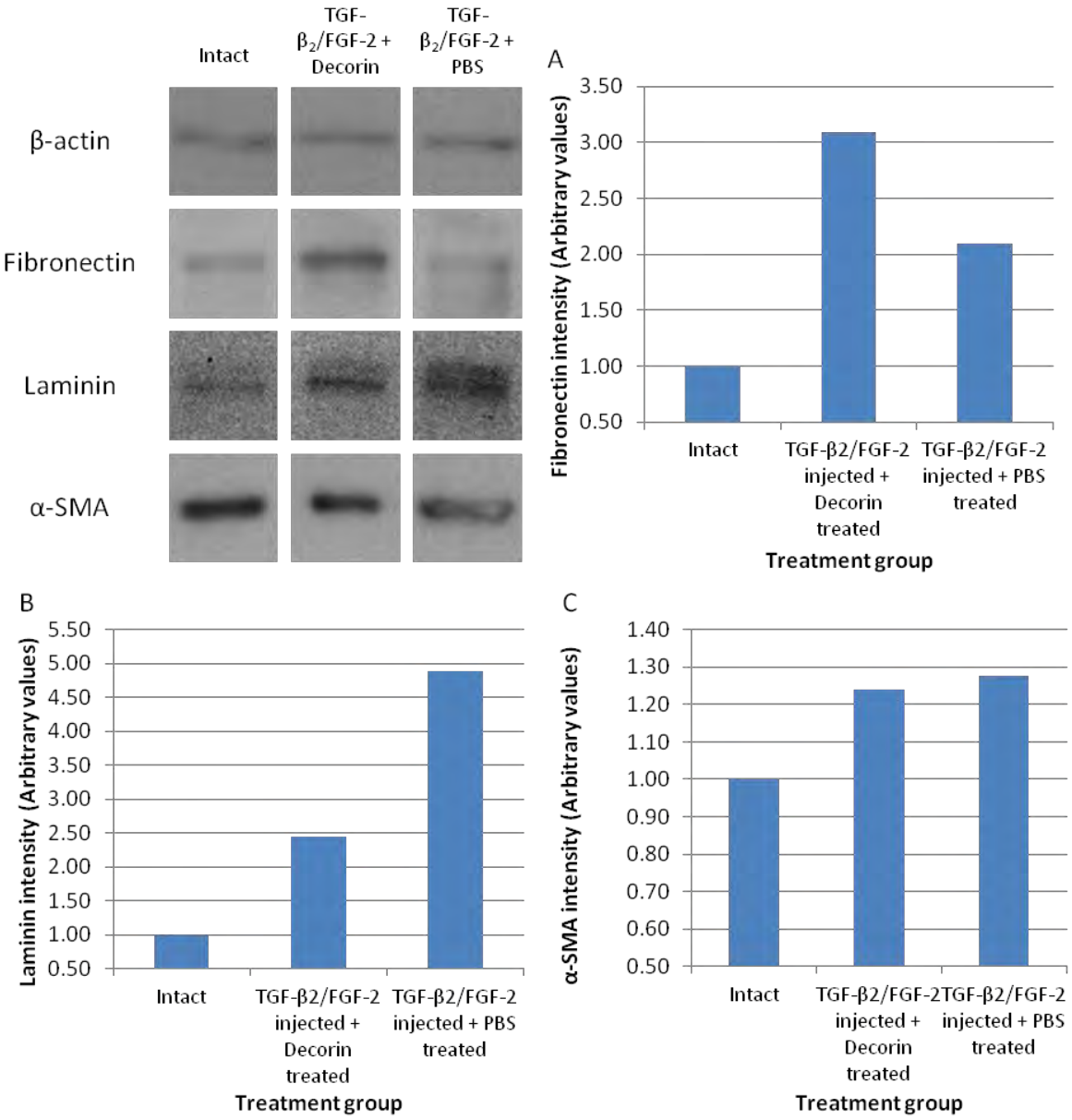

Figure 10: Western blots for animal group 4 that received intravitreal injection of transforming growth factor-β_2/fibroblast growth factor-2 (TGF-β_2/FGF-2) with either intravitreal Decorin treatment (right eye) or intravitreal phosphate-buffered saline (PBS) treatment (left eye). Blots are shown above with densitometric data for fibronectin (A), laminin (B) and α-smooth muscle actin (α-SMA; C) displayed. Data is given as arbitrary values standardised to β-actin loading controls and then to intact eyes. Each treatment group consisted of 4 animals with samples pooled together before blotting.

4 Discussion

4.1 Overview

For quantifying retinal fibrosis, Western blot proved the superior method whereas for immunohistochemistry, identifying areas of fibrosis proved impractical without a defined region of fibrosis to analyse. Western blots performed on animal group 1 showed that a subretinal injection of Healon was able to induce retinal fibrosis, which was evident by the increased fibronectin and laminin density; however no rise in α-SMA was seen. TGF-β_2/FGF-2 intravitreal injection induced no additional fibrosis to Healon injected eyes but did induce a 3-fold increase in α-SMA, indicating an increase in RPE cell differentiation (EMT) into α-SMA$^+$ myofibroblasts. Without a subretinal injection of Healon (group 4), intravitreal injections of TGF-β_2/FGF-2 induced increases in retinal fibronectin and laminin. Bi-weekly injections of Decorin reduced retinal laminin density in this group but increased fibronectin density. No substantial change in α-SMA was seen after intravitreal TGF-β_2/FGF-2 injection, with or without Decorin in this animal group.

4.2 Group 2 and 3

Group 2, which was intravitreally injected with TGF-β_2/FGF-2 in the right eye and PBS in the left eye and group 3, which was the same as group 2 but with bi-weekly Decorin injections beginning at day 14, was analysed immunohistochemically. This proved an impractical method to identify and quantify retinal fibrosis. Gross images of the fundus (Figure 6 and 8) were taken before sectioning and with no observable retinal detachment or fibrosis seen; it seems that only a mild PVR was induced by the growth factor treatments. Immunohistochemical staining (Figure 7 and 9) showed the presence of a laminin$^+$ basement membrane in the retina and GFAP$^+$ glia in the ganglion cell layer while also showing an absence of ED1$^+$ macrophages and α-SMA$^+$ myofibroblasts. Few conclusions can be drawn from the immunohistochemical analysis of these two groups other than an apparent lack of visible inflammation and EMT, which are hallmarks of PVR (Pastor et al., 2002).

4.3 Group 1

Subretinal injection is not a common model of PVR since it induces retinal detachment rather than PVR, despite retinal detachment (even if surgically corrected) being the most common cause of PVR in patients (Pastor, 1998). Where subretinal injection is used as an experimental model, historically, it was to transfect RPE cells to cause expression of a desired growth factor and not to simply detach the retina (Agrawal et al., 2007). In the present study, however, subretinal injection and the resulting retinal detachment increased the fibronectin and laminin density within the retinal tissue (detected by Western blot; Figure 5), an observation seen in PVR patients (Hiscott et al., 1999). The addition of TGF-β_2/FGF-2 did not increase the response so it can be concluded that the retinal fibrosis after retinal detachment, particularly laminin and fibronectin, was not enhanced by exogenous TGF-β_2/FGF-2. This may be due to the retinal detachment itself inducing the release of endogenous TGF-β_2/FGF-2, though without running an assay for these cytokine/growth factors on vitreous from these animals, this is speculative.

Our results demonstrated a substantial increase (3-fold) in α-SMA after intravitreal TGF-β_2/FGF-2 injection compared to intact eyes or those receiving subretinal injection alone. This is not surprising since a previous paper has shown vitreal samples from PVR patients, which have elevated levels of TGF-β, induce contraction of collagen gels and induce a 2.5-fold increase in α-SMA in hyalocytes isolated from the eye (Kita et al., 2008). The increase in α-SMA witnessed in this study was inhibited when antibodies to TGF-β were added but not when fasudil, an inhibitor of the RhoA pathway was used, suggesting the Smad pathway is responsible. Since FGF-2 increases the proliferation of RPE cells and myofibroblasts, it is may also be responsible for the increase in α-SMA/myofibroblasts (Pastor, 1998).

As mentioned previously, α-SMA$^+$ myofibroblasts derive from RPE cells by a special type of differentiation known as EMT. A previous paper has shown RPE cells undergo EMT in response to TGF-β both *in vitro* and *in vivo* (Saika et al., 2004). The authors attributed this to the Smad pathway

by firstly showing TGF-β activated the Smad pathway within 30 minutes of administration and secondly, using Smad3-knockout mice to completely prevent both the EMT and the enhanced α-SMA expression. In a similar study the authors inhibited EMT by over expressing Smad7, an inhibitor in the Smad pathway (Saika et al., 2007).

Since α-SMA$^+$ myofibroblasts are so important in PVR by transforming a regular retinal detachment into a tractional retinal detachment (Pastor et al., 2002) it can be said that injecting TGF-β_2/FGF-2 intravitreally alongside the subretinal Healon injection is the better model of PVR in comparison to the subretinal injection alone. This leaves the question as to how a retinal detachment in patients induces EMT and if it is through inducing the release of endogenous TGF-β, why has it not done so in this particular model.

4.4 Group 4

The observation that intravitreal TGF-β_2/FGF-2 induced retinal fibrosis, assessed by Western blot (Figure 10), corroborates what is previously known, that PVR patients have increased concentrations of TGF-β_2 in the vitreous (Connor et al., 1989) and suggests that this correlation is causative. Although Decorin, an anti-fibrotic agent was able to reduce laminin density by 2-fold, paradoxically, Decorin further increased fibronectin density over the initial increase induced by TGF-β_2/FGF-2. This is in direct conflict with previous work that shows Decorin reduces TGF-β-induced fibronectin production in the cornea (Mohan et al., 2010).

Interestingly, intravitreal TGF-β_2/FGF-2 injection did not increase α-SMA expression like it did in group 1, suggesting that retinal detachment is a required factor in TGF-β_2-induced EMT. Since the two previous papers (Saika et al., 2004; Saika et al., 2007) showing TGF-β_2-induced EMT also used retinal detachment as their model, it is likely that retinal detachment is required, possibly to allow TGF-β_2 to act on the RPE cells situated underneath the retina. However, one study refutes this contention by showing that, although vitreal TGF-β_2 correlates with PVR in patients, high levels of

TGF-β_2 in the subretinal fluid protect against PVR (Dieudonne et al., 2004). This paper would argue that whatever TGF-β is interacting with to induce or augment PVR, its interactions cannot be with RPE cells since they are in direct contact with the subretinal fluid.

Due to lack of elevated α-SMA, we were unable to test Decorin's efficacy at reducing any α-SMA overexpression, which is an effect we would have expected. This expectation is based on previous research in the cornea whereby TGF-β-induced EMT was prevented by transfecting corneal fibroblasts to express Decorin (Mohan et al., 2010).

4.5 Future work

Unfortunately, due to technical issues and limited time, a non-denatured Western blot was not performed adequately and as such, this remains an important future experiment to determine further the extent of fibrosis in this model. Previous papers have shown that RPE cells produce collagen I in response to TGF-β in a Smad dependant fashion (Saika et al., 2007) and so, similar to what is seen with laminin, collagen would be expected to increase in the TGF-β_2/FGF-2 treated groups and to be attenuated in the groups receiving Decorin. Repeats of standard, denatured Western blots will also need to be done to obtain enough data to perform statistical tests. This may also remove some of the paradoxical results seen, such as Decorin increasing fibronectin density.

More markers of fibrosis and epiretinal membrane formation are available and analysis of these and how they change in this model is an important future experiment. One example is GFAP since, as mentioned previously, $GFAP^+$ glial cells are an important contributor to wound healing in the CNS and retina and make up a significant part of the cellular component of epiretinal membranes (Pastor et al., 2002). A recent study used TGF-β antibodies to inhibit PVR in a mouse model and significantly reduce fibrosis, while interestingly, only using GFAP as a marker for subretinal fibrosis (Zhang and Liu, 2012). Other markers involved in fibrosis and remodelling are matrix metalloproteinases (MMP)

of which, MMP-2 and MMP-9 were found at significantly high levels in PVR patients that were correlated with the development of postoperative PVR (Kon et al., 1998).

Since subretinal Healon and intravitreal TGF-β_2/FGF-2 injection worked best at inducing measurable retinal fibrosis, evident by the increase in fibrotic markers (fibronectin and laminin) and markers of EMT (α-SMA) by Western blot, the next stage would be to assess Decorin as a suitable treatment in this particular model. One such paper has already done preliminary work in assessing Decorin as a treatment option for PVR (Nassar et al., 2011). Using a retinal injury-induced animal model of PVR, they showed a smaller fibrosed area and a reduction in grade of PVR on a clinical grading scale (performed by an Ophthalmologist). As well as corroborating our findings of decreased fibrosis they also performed an examination for any drug related toxicity and found none, thus suggesting Decorin to be a safe future drug. Unfortunately, they failed to look for key fibrotic proteins and assess their protein expression, as was done in this study, and thus key conclusions such as the extent of EMT and changes in individual protein levels are not possible.

In this present study we have assumed that subretinal injection of Healon led to retinal detachment, however, this assumption was never verified. With *in vivo* imaging techniques, such as a scanning laser ophthalmoscope and an optical coherence tomography machine, it would be possible to view retinal detachment *in vivo* (Cebulla et al., 2010) and accurately quantify it. This is more reliable than trying to visualize retinal detachment after the animal is sacrificed since the process of tissue preparation gives rise to artefacts.

An important consideration is how translational Decorin is as a treatment. If found to have efficacy in treating PVR then, along with its good safety profile, an effective form of intravitreal delivery will need to be established that will avoid repeated intravitreal injections. One such study used a long term delivery method with microspheres containing the anti-proliferative agent retinoic acid in a rabbit model of PVR (Giordano et al., 1993). They showed that following a single injection of the microspheres, drug release remained constant for 30 days and thus bypassing the need for repeated

intravitreal injections. A similar method allowing the sustained release of Decorin would overcome the impractical bi-weekly intravitreal injections and is necessary for clinical trials.

Finally, an important consideration is the time frame of the study, and how long animals need to be left following retinal detachment and/or TGF-β_2/FGF-2 injection before a mature scar forms. In the present study animals were left for 28 days however, areas of haemorrhage were seen in the eyes, suggesting fibrosis was still in its early stages and thus, a longer time frame is needed before a scar and possibly epiretinal membranes form.

4.6 Conclusion

Two important conclusions can be drawn from this study. The first is that immunohistochemistry is a substandard method for quantifying fibrosis, particularly in PVR where no isolated region can be analysed. Future experiments should concentrate on Western blots and possibly PCR to reliably quantify changes in retinal fibrosis related proteins.

The second conclusion is that subretinal injection of Healon induces retinal fibrosis, and when coupled with TGF-β_2/FGF-2, also induces EMT and the formation of myofibroblasts. Based on our limited assessment of markers for fibrosis and PVR, this proved to be the best model of PVR for future use. Decorin, although showing promise in being able to reduce laminin density by a half, remains untested in our preferred model. Future work concentrating on one particular model, Decorin's effects on this model and a larger array of PVR related protein changes analysed by Western blot will, (1), shed light on the pathogenesis of PVR in our model and, (2), provide stronger evidence of Decorin's potential as a treatment for PVR.

5 References

Agrawal, R.N., He, S., Spee, C., Cui, J.Z., Ryan, S.J., Hinton, D.R., 2007. In vivo models of proliferative vitreoretinopathy. Nature Protocols 2, 67-77.

Berkowitz, B.A., Lukaszew, R.A., Mullins, C.M., Penn, J.S., 1998. Impaired hyaloidal circulation function and uncoordinated ocular growth patterns in experimental retinopathy of prematurity. Investigative Ophthalmology & Visual Science 39, 391-396.

Berry, M., Ahmed, Z., Lorber, B., Douglas, M., Logan, A., 2008. Regeneration of axons in the visual system. Restorative Neurology and Neuroscience 26, 147-174.

Blobe, G.C., Schiemann, W.P., Lodish, H.F., 2000. Mechanisms of disease: Role of transforming growth factor beta in human disease. New England Journal of Medicine 342, 1350-1358.

Border, W.A., Noble, N.A., Yamamoto, T., Harper, J.R., Yamaguchi, Y., Pierschbacher, M.D., Ruoslahti, E., 1992. Natural Inhibitor of Transforming Growth-Factor-Beta Protects against Scarring in Experimental Kidney-Disease. Nature 360, 361-364.

Brar, M., Bartsch, D.U.G., Nigam, N., Mojana, F., Gomez, L., Cheng, L., Hedaya, J., Freeman, W.R., 2009. Colour versus grey-scale display of images on high-resolution spectral OCT. British Journal of Ophthalmology 93, 597-602.

Cassidy, L., Barry, P., Shaw, C., Duffy, J., Kennedy, S., 1998. Platelet derived growth factor and fibroblast growth factor basic levels in the vitreous of patients with vitreoretinal disorders. British Journal of Ophthalmology 82, 181-185.

Cebulla, C.M., Ruggeri, M., Murray, T.G., Feuer, W.J., Hernandez, E., 2010. Spectral domain optical coherence tomography in a murine retinal detachment model. Experimental Eye Research 90, 521-527.

Charteris, D.G., 1995. Proliferative Vitreoretinopathy - Pathobiology, Surgical-Management, and Adjunctive Treatment. British Journal of Ophthalmology 79, 953-960.

Charteris, D.G., Sethi, C.S., Lewis, G.P., Fisher, S.K., 2002. Proliferative vitreoretinopathy - developments in adjunctive treatment and retinal pathology. Eye 16, 369-374.

Connor, T.B., Roberts, A.B., Sporn, M.B., Danielpour, D., Dart, L.L., Michels, R.G., Debustros, S., Enger, C., Kato, H., Lansing, M., Hayashi, H., Glaser, B.M., 1989. Correlation of Fibrosis and Transforming Growth Factor-Beta Type-2 Levels in the Eye. Journal of Clinical Investigation 83, 1661-1666.

Cook, B., Lewis, G.P., Fisher, S.K., Adler, R., 1995. Apoptotic Photoreceptor Degeneration in Experimental Retinal-Detachment. Investigative Ophthalmology & Visual Science 36, 990-996.

Derynck, R., Zhang, Y.E., 2003. Smad-dependent and Smad-independent pathways in TGF-beta family signalling. Nature 425, 577-584.

Dieudonne, S.C., La Heij, E.C., Diederen, R., Kessels, A.G.H., Liem, A.T.A., Kijlstra, A., Hendrikse, F., 2004. High TGF-beta 2 levels during primary retinal detachment may protect against proliferative vitreoretinopathy. Investigative Ophthalmology & Visual Science 45, 4113-4118.

Fukui, N., Fukuda, A., Kojima, K., Nakajima, K., Oda, H., Nakamura, K., 2001. Suppression of fibrous adhesion by proteoglycan decorin. Journal of Orthopaedic Research 19, 456-462.

Gilbert, C., Hiscott, P., Unger, W., Grierson, I., Mcleod, D., 1988. Inflammation and the Formation of Epiretinal Membranes. Eye 2, S140-S156.

Giordano, G.G., Refojo, M.F., Arroyo, M.H., 1993. Sustained Delivery of Retinoic Acid from Microspheres of Biodegradable Polymer in Pvr. Investigative Ophthalmology & Visual Science 34, 2743-2751.

Graw, J., 2003. The genetic and molecular basis of congenital eye defects. Nature Reviews Genetics 4, 876-888.

Grisanti, S., Szurman, P., Warga, M., Kaczmarek, R., Ziemssen, F., Tatar, O., Bartz-Schmidt, K.U., 2005. Decorin modulates wound healing in experimental glaucoma filtration surgery: A pilot study. Investigative Ophthalmology & Visual Science 46, 191-196.

Hiscott, P., Sheridan, C., Magee, R.M., Grierson, I., 1999. Matrix and the retinal pigment epithelium in proliferative retinal disease. Progress in Retinal and Eye Research 18, 167-190.

Iozzo, R.V., 1997. The family of the small leucine-rich proteoglycans: Key regulators of matrix assembly and cellular growth. Critical Reviews in Biochemistry and Molecular Biology 32, 141-174.

Kita, T., Hata, Y., Arita, R., Kawahara, S., Miura, M., Nakao, S., Mochizuki, Y., Enaida, H., Goto, Y., Shimokawa, H., Hafezi-Moghadam, A., Ishibashi, T., 2008. Role of TGF-beta in proliferative vitreoretinal diseases and ROCK as a therapeutic target. Proceedings of the National Academy of Sciences of the United States of America 105, 17504-17509.

Kon, C.H., Occleston, N.L., Charteris, D., Daniels, J., Aylward, G.W., Khaw, P.T., 1998. A prospective study of matrix metalloproteinases in proliferative vitreoretinopathy. Investigative Ophthalmology & Visual Science 39, 1524-1529.

Logan, A., Ahmed, Z., Baird, A., Gonzalez, A.M., Berry, M., 2006. Neurotrophic factor synergy is required for neuronal survival and disinhibited axon regeneration after CNS injury. Brain 129, 490-502.

Logan, A., Baird, A., Berry, M., 1999. Decorin attenuates gliotic scar formation in the rat cerebral hemisphere. Experimental Neurology 159, 504-510.

Machemer, R., 1988. Proliferative Vitreoretinopathy (Pvr) - a Personal Account of Its Pathogenesis and Treatment - Proctor Lecture. Investigative Ophthalmology & Visual Science 29, 1771-1783.

Mccormack, P., Simcock, P.O.R., Charteris, D., Lavin, M.J., 1994. Is Surgery for Proliferative Vitreoretinopathy Justifiable. Eye 8, 75-76.

Mohan, R.R., Gupta, R., Mehan, M.K., Cowden, J.W., Sinha, S., 2010. Decorin transfection suppresses profibrogenic genes and myofibroblast formation in human corneal fibroblasts. Experimental Eye Research 91, 238-245.

Nassar, K., Luke, J., Luke, M., Kamal, M., Abd El-Nabi, E., Soliman, M., Rohrbach, M., Grisanti, S., 2011. The novel use of decorin in prevention of the development of proliferative vitreoretinopathy (PVR). Graefes Archive for Clinical and Experimental Ophthalmology 249, 1649-1660.

Pastor, J.C., 1998. Proliferative vitreoretinopathy: An overview. Survey of Ophthalmology 43, 3-18.
Pastor, J.C., de la Rua, E.R., Martin, F., 2002. Proliferative vitreoretinopathy: risk factors and pathobiology. Progress in Retinal and Eye Research 21, 127-144.

Pena, R.A., Jerdan, J.A., Glaser, B.M., 1994. Effects of Tgf-Beta and Tgf-Beta Neutralizing Antibodies on Fibroblast-Induced Collagen Gel Contraction - Implications for Proliferative Vitreoretinopathy. Investigative Ophthalmology & Visual Science 35, 2804-2808.

Rolls, A., Shechter, R., Schwartz, M., 2009. NEURON - GLIA INTERACTIONS - OPINION The bright side of the glial scar in CNS repair. Nature Reviews Neuroscience 10, 235-U291.

Saika, S., Kono-Saika, S., Tanaka, T., Yamanaka, O., Ohnishi, Y., Sato, M., Muragaki, Y., Ooshima, A., Yoo, J., Flanders, K.C., Roberts, A.B., 2004. Smad3 is required for dedifferentiation of retinal pigment epithelium following retinal detachment in mice. Laboratory Investigation 84, 1245-1258.

Saika, S., Yamanaka, O., Nishikawa-Ishida, I., Kitano, A., Flanders, K.C., Okada, Y., Ohnishi, Y., Nakajima, Y., Ikeda, K., 2007. Effect of Smad7 gene overexpression on transforming growth factor beta-induced retinal pigment fibrosis in a proliferative vitreoretinopathy mouse model. Archives of Ophthalmology 125, 647-654.

Shafiee, A., McIntire, G.L., Sidebotham, L.C., Ward, K.W., 2008. Experimental determination and allometric prediction of vitreous volume, and retina and lens weights in Gottingen minipigs. Veterinary Ophthalmology 11, 193-196.

Yamaguchi, Y., Mann, D.M., Ruoslahti, E., 1990. Negative Regulation of Transforming Growth-Factor-Beta by the Proteoglycan Decorin. Nature 346, 281-284.

Zhang, H., Liu, Z.L., 2012. Transforming growth factor -beta neutralizing antibodies inhibit subretinal fibrosis in a mouse model. International Journal of Ophthalmology 5, 307-311.